2017

A comparison of computational methods for estimating estuarine production and respiration from diel open water dissolved oxygen measurements

Spencer Tassone
Virginia Commonwealth University

A COMPARISON OF COMPUTATIONAL METHODS FOR ESTIMATING ESTUARINE PRODUCTION AND RESPIRATION FROM DIEL OPEN WATER DISSOLVED OXYGEN MEASUREMENTS

A thesis submitted in partial fulfillment of the requirements for the
Degree of Master of Science in Biology at Virginia Commonwealth University

by

Spencer J. Tassone
BS in Environmental Studies, Virginia Commonwealth University, 2014
AS in Social Sciences, Tidewater Community College, 2011

Advisor: Dr. Paul A. Bukaveckas
Professor, VCU Department of Biology and Center for Environmental Studies

Virginia Commonwealth University
Richmond, Virginia
July, 2017

Acknowledgments

I would like to thank my family and friends for their help and support throughout my academic career. I would like to express my gratitude to Dr. Alison Appling for her patience and help with the Bayesian modelling component of this study. This project would not have been possible without the assistance of William Lee (method training, sonde calibration and CHLa analysis), David Hopler (field assistance), Dana Devore (field assistance) and Lara Whitlow (field assistance). A special thanks to the VCU Rice Rivers Center, my committee and my advisor Dr. Paul Bukaveckas for his patience, support and guidance over the past 5 years.

Table of Contents

Abstract

A COMPARISON OF COMPUTATIONAL METHODS FOR ESTIMATING ESTUARINE PRODUCTION AND RESPIRATION FROM DIEL OPEN WATER DISSOLVED OXYGEN MEASUREMENTS

By: Spencer J. Tassone, M.S.

A thesis submitted in partial fulfillment of the requirements for the degree of Master of Science in Biology at Virginia Commonwealth University.

Virginia Commonwealth University, 2017.

Advisor: Dr. Paul A. Bukaveckas, Professor, VCU Department of Biology and Center for Environmental Studies

Diel dissolved oxygen (DO) data were used to characterize seasonal, inter-annual, and longitudinal variation in production and respiration for the James River Estuary. Two computational methods (Bayesian and bookkeeping) were applied to these data to determine whether inferences regarding DO metabolism are sensitive to methodology. Net metabolism was sensitive to methodology as Bayesian results indicated net heterotrophy (production < respiration) while bookkeeping results indicated net autotrophy (production > respiration). Differences in net metabolism among the methods was due to low seasonal variation in respiration using the Bayesian method, whereas bookkeeping results showed a strong correlation between production and respiration. Bayesian results suggest a dependence on allochthonous organic matter (OM) whereas bookkeeping results suggest that metabolism is dependent on autochthonous OM. This study highlights the importance in considering the method used to derive metabolic estimates as it can impact the assessment of trophic status and sources of OM supporting an estuary.

Introduction

Ecosystem ecologists have long been interested in primary production because of the important role that primary producers play in elemental cycles and in food web energetics (Lindeman 1942, Odum 1956). Recent interest in this topic has sought to place gross primary production (GPP) in the broader context of ecosystem metabolism, i.e., the balance between organic matter (OM) production via photosynthesis and OM consumption via autotrophic and heterotrophic respiration (ecosystem respiration; hereafter, ER). In aquatic systems, interest in net ecosystem metabolism (NEM = GPP-ER) has reflected in part a desire to understand the role of subsidies (allochthonous OM inputs) in supporting ecosystem metabolism, and to characterize aquatic systems as being net sources or sinks in the context of the global carbon cycle (i.e., net autotrophic (GPP > ER) or heterotrophic (ER > GPP); Vannote et al. 1980, Borges 2005, Tranvik et al. 2009, Raymond et al. 2013, Houser et al. 2015, Hall et al. 2016). Interest in aquatic ecosystem metabolism has also been fueled by technological advances in autonomous monitoring of dissolved oxygen (DO), which allow for characterization of ecosystem metabolism over larger spatial and temporal scales, and by computational advances in the means by which these data are analyzed (e.g., Bayesian methods).

Among aquatic ecosystems, estuaries rank among the most metabolically active due to their high rates of production and respiration (Hoellein et al. 2013). Estuaries receive large external inputs of OM and nutrients from terrestrial, marine and freshwater sources. High rates of respiration are supported by allochthonous OM from the catchment and nutrient inputs, which elevate primary production and provide labile OM (Vincent et al. 1996, Kemp et al. 1997, Muylaert et al. 2005, Hoellein et al. 2013). Production and respiration are often correlated, but seasonal, inter-annual and longitudinal factors can shift the balance between GPP and ER.

Seasonal differences in water temperature and photosynthetically active radiation (PAR) impact the rate of production and respiration in estuaries, with greatest GPP and ER during summer and lowest rates during winter (Cory et al. 1974, Boynton et al. 1982, Cole et al. 1992, D'vanzo et al. 1996, Caffrey 2014). Seasonal variation in runoff affects the timing of OM and nutrient inputs as well as advective transport of plankton (Paerl et al. 2010, Bruesewitz et al. 2013, Caffrey et al. 2014, Cloern et al. 2014). Longitudinal variation in salinity and channel morphometry influences plankton community development (Boynton et al. 1982, Kemp et al. 1997, Paerl et al. 2010, Roelke et al. 2017) and the balance between heterotrophy and autotrophy (Smith and Kemp 1995, Kemp et al. 1997, Raymond et al. 2000, Caffrey 2004). A recent review of 5 inter-annual and 11 spatial estuarine productivity studies showed that production can vary 5-fold inter-annually and 10-fold spatially within an estuary (Cloern et al. 2014 and references therein). Kemp et al. (1997) showed distinct changes in the balance between production and respiration within Chesapeake Bay, with the oligohaline segment (0.5-5 ppt) being annually net heterotrophic, and the polyhaline segment (18+ ppt) being net autotrophic. A recent meta-analysis of 48 estuaries found 11% of estuaries to be annually net autotrophic and 89% to be net heterotrophic (Hoellein et al. 2013), suggesting that most annual production is respired within estuaries and that allochthonous inputs to estuaries routinely drive respiration rates in excess of production.

A key challenge in estimating ecosystem-scale production and respiration is properly accounting for non-biological oxygen fluxes (i.e., atmospheric exchange; hereafter, AE). AE is regulated by the concentration gradient between air and water (i.e., dissolved oxygen saturation), and by the gas transfer velocity (Deacon 1981, Wanninkhof 1992, Hopkinson and Smith 2005, Raymond et al. 2012). Gas transfer velocity is determined in part by boundary layer thickness,

which is influenced by wind speed and water velocity (Wanninkhof 1992, Holtgrieve et al. 2010, Raymond et al. 2012). In lentic systems (i.e., lakes) and oceans, boundary layer thickness is largely determined by wind speed due to large fetch and the absence of fluvial and tidal mixing (Deacon 1981, Wanninkhof 1992, Marino and Howarth 1993). Lotic systems (i.e., streams and rivers) typically have higher rates of gas exchange due to their low surface area to volume ratio and higher water velocity (Raymond et al. 2012). Within estuaries there is a complex interaction of factors acting on gas exchange including tidal forces (which are dependent on tidal amplitude and channel morphometry), fluvial forces (which vary longitudinally, and with discharge) and wind-driven mixing forces (which are influenced by fetch and climatic conditions; Ho et al. 2011, Crosswell et al. 2012). A further complicating factor is that the surface area to volume ratio of estuaries is variable, both longitudinally and over time (due to the influence of tides, and sea-surface elevation). While quantifying AE in estuaries presents a challenge, it is not well understood how sensitive metabolism estimates are to various methods of determining AE (Odum 1956, Caffrey 2003, Fahey and Knapp 2007, Hondzo et al. 2013).

Numerous methods have been developed to estimate aquatic metabolism and AE based on open measurements, particularly for lake and stream environments. A common method uses a 'bookkeeping' approach of tracking incremental changes in DO over a diel cycle. Caffrey (2003, 2004) used this method to analyze diel oxygen data from 42 estuaries that were part of NERRS (National Estuarine Research Reserve System) (hereafter, Caffrey Method). This method ascribes increases in DO during the day to production, decreases in DO during night to respiration, and calculates AE as the product of the concentration gradient of O_2 between air-water and a fixed exchange coefficient. The advantage of this method is that it requires minimal parameterization, and, as it has been applied to a large number of estuaries, provides a basis for

comparing oxygen metabolism across systems (Caffrey 2003, 2004, Hoellein et al. 2013). However, this method does not account for the effects of wind speed or water velocity on AE and can potentially provide artificial ecological processes (e.g., negative GPP; Caffrey 2003, Winslow et al. 2016). As wind, fluvial and tidal influences on AE are likely to vary over time and longitudinally, this may lead to biased estimates of GPP, ER and NEM.

Recent studies have applied Bayesian analyses to assess uncertainty in metabolism estimates, inclusive of observation uncertainty (measurement precision and accuracy), process uncertainty (stochasticity of model parameters), and model uncertainty. By this method unmeasured metabolic parameters (i.e., GPP, ER, AE) and associated parameter uncertainty (i.e., standard deviation; hereafter, SD) are treated as random variables with prior information (mean ± SD; hereafter, priors) on their distribution (Holtgrieve et al. 2010, Grace et al. 2015, Hall et al. 2016, Winslow et al. 2016). The program 'streamMetabolizer' uses a Bayesian approach to inverse modeling, which fits a numerical model describing oxygen gains and losses to input data (e.g., DO measurements). Bayesian analyses are a useful alternative to the bookkeeping approach as they offer uncertainty estimates for modeled parameters (GPP and ER) and can accommodate variable rates of atmospheric exchange arising from differences in wind, fluvial and tidal forcing (Soloman et al. 2013, Hall et al. 2016, Winslow et al. 2016). However, Bayesian analyses require prior information about a system, and are computationally intensive (Grace et al. 2015, Winslow et al. 2016). While both the Caffrey and Bayesian methods estimate metabolic parameters and AE using the same input data (diel oxygen measurements), they offer different approaches to deriving those estimates. A key unresolved question is, are metabolic estimates influenced over time (i.e., seasonally, inter-annually) and/or space (i.e., longitudinally) due to methodological choice?

We analyzed 23 years of DO data from stations located within the James River Estuary (JRE) to better understand seasonal, inter-annual and longitudinal variation in production, respiration and net ecosystem metabolism. Metabolic estimates were derived using both the Caffrey and Bayesian methods to determine whether inferences about seasonal, inter-annual and longitudinal patterns were sensitive to methodological influences. Relationships between metabolic estimates derived using both methods were used to test relationships with environmental variables (i.e., pelagic metabolism, PAR and water temperature) and to make inferences about sources of OM supporting metabolism. Results from these analyses were used to address two questions: (1) How does the balance between production and respiration (i.e., NEM) vary seasonally, inter-annually and longitudinally within the estuary? and (2) Is our assessment of seasonal and spatial patterns in net ecosystem metabolism sensitive to the methods used to derive GPP and ER?

Methods and Materials

Study Site

The James River is the third largest and southern most of the 5 major tributaries of Chesapeake Bay. It drains a mountainous catchment (watershed area = 26,101 km^2) comprised of 67% forest, 20% agriculture, 12% urban and 1% wetland (Bricker et al. 2007). The James River has a total length of 545 km, of which the lower third is tidal extending from the Fall Line in Richmond, VA to the confluence with Chesapeake Bay (Fig. 1). The JRE is divided into segments based on salinity: tidal fresh (TF, 0-0.5 ppt), oligohaline (OH, 0.5-5 ppt), mesohaline (MH, 5-18 ppt) and polyhaline (PH, 18+ ppt) (USEPA Chesapeake Bay Program Office 2005). The TF segment is further divided into upper and lower segments which differ in their geomorphology. The upper section, located between the Fall Line and the confluence with the

Appomattox River, has a riverine morphometry with a deep (> 3 m), constricted channel and low ratio of photic depth to total depth (Bukaveckas et al. 2011, Wood and Bukaveckas 2014). The lower TF section extends to the Chickahominy River, and is characterized by a more estuarine morphometry, with shallow (< 3 m) depths, a broader channel, and more favorable light conditions (Bukaveckas et al. 2011, Wood and Bukaveckas 2014). Continuous water quality monitoring data were collected at a station located in the lower tidal fresh segment (Virginia Commonwealth University Rice Rivers Center; VCU RRC) during 2009-2016, and at stations located in each of the 5 salinity segments during March-November of 2006-2008 (Table 1; Virginia Institute of Marine Science, Virginia Estuarine and Coastal Observing System; VECOS). The VECOS dataset was selected for analysis because it allows for estimation of ecosystem metabolism over a range of estuarine conditions from tidal freshwater to polyhaline. The Rice Pier dataset was selected as it provides long-term (8-years) data collected year-round. Thus, a total of 23 station-years of continuous monitoring data were available to assess seasonal, inter-annual and inter-segment differences in DO metabolism.

Ecosystem Metabolism

Daily rates of ecosystem GPP, ER and AE were derived using one-station open water diel O_2 curves derived from 15-minute measurements. All data were collected with optical oxygen probes using YSI 6600 water quality sondes (2006-2014) or YSI EXO2 water quality sondes (2015-2016). Sondes were calibrated every 3 weeks. An important assumption when determining metabolic rates using the single station method is that tidal exchange does not influence local DO concentrations (Cole et al. 2000, Caffrey 2003). Previous analysis in the JRE has shown that tidal exchange does not explain a significant proportion of the residual variation in DO concentration (Bukaveckas et al. 2011).

Caffrey Method

Following Caffrey (2003, 2004), 15-minute DO measurements (g m^{-3}) were smoothed to 30-minute averages and multiplied by water depth (m) to obtain areal rates of oxygen flux, which were summed across 24-hour periods (g O_2 m^{-2} d^{-1}; Equation 1). DO fluxes during daylight hours were considered net primary production (NPP), while ER was derived by extrapolating nightly O_2 fluxes to a 24-hour period. GPP was derived based on the sum of NPP + ER during daylight hours, and NEM was derived by subtracting daily ER from GPP.

$$O_2 \text{ flux} = (DO_{t_2} - DO_{t_1}) * \text{Water Depth} - AE \qquad (1)$$

For this analysis, a fixed average depth was used (i.e., without consideration for seasonal and tidal variation in water surface elevation). Average depths for the five segments were: upper TF = 2.7 m, lower TF = 2.5 m, OH = 3.1 m, MH = 3.1 m and PH = 5.6 m (USEPA Chesapeake Bay Program Office 2005).

$$AE = \left(1 - \frac{DO_{sat,t_2} + DO_{sat,t_1}}{200}\right) * 0.5 * \Delta t \qquad (2)$$

AE was derived based on DO measurements (as % saturation) that were multiplied by a fixed gas transfer coefficient (0.5 g O_2 m^{-2} h^{-1}; Equation 2). The Caffrey method assumes that AE is affected solely by the air-water concentration gradient and thus varies between -0.5 to 0.5 g O_2 m^{-2} h^{-1} when water column saturation is between 0-200%.

Bayesian Method

The Bayesian analysis of estuarine metabolism was performed using the modeling package 'streamMetabolizer' (version 0.9.33; Table 2; Appling et al. 2017, R Core Team 2017). Bayesian modeling estimates unmeasured metabolic parameters (θ; i.e., GPP and ER) using a known prior probability ($P(\theta)$) distribution (mean and SD) of θ, and a vector of measured input parameters (D; i.e., DO concentration, DO saturation (determined via water temperature), day

length (determined via PAR) and depth; Equation 3; Hobbs and Hooten 2015, Hall et al. 2016). The likelihood ($P(D|\theta)$) of the measured input data given our prior estimates of θ is proportional to the posterior distribution, $P(\theta|D)$ of θ from which estimates of our unmeasured metabolic parameters are derived.

$$P(\theta|D) \propto P(D|\theta) * P(\theta) \qquad (3)$$

The Bayesian analysis was performed using estuarine specific priors for GPP and ER, site-specific priors for AE and locally measured tidal variation in depth. Tidal variation in depth was determined by detrending the recorded depth from sonde measurements and adding the average segment depth to the detrended depth measurements. Priors for GPP and ER are available via streamMetabolizer but these are generic values (not estuarine specific) representing previous applications, many of which were small stream studies. We obtained estuarine specific priors that represent summer conditions for 44 estuarine sites (Hoellein et al. 2013). From these data, we derived the mean and standard deviation of GPP (μ = 10.8 g O_2 m^{-2} d^{-1}, σ = 6.7 g O_2 m^{-2} d^{-1}) and ER (μ = 13.6 g O_2 m^{-2} d^{-1}, σ = 7.4 g O_2 m^{-2} d^{-1}). Site-specific estimation of AE required estimates of k_{600} (daily reaeration rate; d^{-1}) which were derived utilizing a segment-specific average (2006-2013) gas transfer velocity (k_{O_2}; m d^{-1}) obtained from the tidal James River hydrodynamic model (Shen et al. 2016). The James River hydrodynamic model uses an additive combination of the effects of wind speed (monitored at Richmond and Norfolk airports), using the Thomann and Mueller formula (Thomann and Mueller 1987), and water velocity, using the O'Connor-Dobbins formula (O'Connor and Dobbins 1958) to derive k_{O_2}. AE was then derived for each 15-minute measurement as k_{O_2} multiplied by the difference between DO saturation and modeled DO.

Model derived k_{O_2} values averaged 1.12, 1.48, 1.05, 1.67 and 1.33 m d^{-1} for the upper and lower TF, OH, MH and PH segments of the JRE respectively. Site-specific k_{600} priors were then derived by normalizing the temperature dependent Schmidt number (Sc_{O_2}), which relates gas solubility to water viscosity in flowing freshwater ecosystems, to 600. The normalized Sc_{O_2} is then raised to the power of -0.5 due to wind-induced surface water turbulence (Jähne et al. 1987), and multiplied by the site-specific average k_{O_2} (Equation 4, Raymond et al. 2012).

$$k_{600} = (600/ Sc_{O_2})^{-0.5} * k_{O_2} \qquad (4)$$

After log-transforming the derived k_{600} values, site-specific k_{600} priors for the lower TF James from 2009-2016 were $\mu = 0.39$ d^{-1}, $\sigma = 0.23$ d^{-1}. Log transformed site-specific k_{600} priors for each of the 5 salinity segments from 2006-2008 were -0.06 ± 0.15 (upper TF), 0.27 ± 0.16 (lower TF), -0.09 ± 0.13 (OH), 0.39 ± 0.13 (MH) and 0.22 ± 0.17 d^{-1} (PH).

In order to assess the sensitivity of Bayesian metabolism estimates to the effects of variable depth and the selection of priors, three alternative modeling scenarios were performed with the 2009-2016 data from the lower TF James (Fig. 2). The first alternative Bayesian model (AB1) used estuarine-specific priors for GPP and ER, and segment-specific priors for AE but with a constant depth equal to the average depth of the lower TF segment (2.5 m) (i.e., without tidal driven variation in depth; similar to Caffrey Method). The second alternative Bayesian model (AB2) used the estuarine specific priors for GPP and ER, but with the generic streamMetabolizer log k_{600} prior (1.79 ± 1 d^{-1}). The third Bayesian model scenario (AB3) used generic streamMetabolizer priors for GPP and ER (8 ± 4 and 10 ± 5 g O_2 m^{-2} d^{-1} respectively) with the segment-specific priors for k_{600}. Results from the three alternative scenarios were compared to the Bayesian and Caffrey model results.

Pelagic Metabolism

Pelagic production and respiration were measured to determine their relative contributions to ecosystem production and respiration. Pelagic metabolism was measured during 2015-2016 at stations located in the upper and lower tidal fresh segments using the light-dark bottle technique (Carignan et al. 1998). Light bottles measure net production of oxygen via photosynthesis (P in excess of R), while dark bottles measure respiration (i.e., oxygen consumption). Surface water samples were collected at Osborne Landing (upper TF) and the VCU RRC (lower TF) twice per month when water temperatures were > 10 °C and once per month when water temperatures were < 10 °C. Light and dark bottles were incubated for 2 and 24 hours respectively. Sufficient incubation time is needed to produce measurable changes in DO. Preliminary experiments showed non-linear effects (reduced hourly rates of metabolism) when incubation lengths in light bottles exceeded 2 hours. DO concentrations were measured using the micro-Winkler technique to obtain a precision ~0.01 mg O_2 L^{-1} (Carignan et al. 1998, Bukaveckas et al. 2011). The change in DO from the start to the end of the incubation was used to determine Net Primary Production (NPP; light bottles), R (dark bottles) and GPP (as NPP + R).

Water collected from the upper and lower TF sites was incubated in situ at the VCU RRC pier. Triplicate bottles (60 mL BOD) were incubated at 0.5 m depth intervals within the photic zone (0-2.0 m). Production versus irradiance curves were derived to estimate pelagic production throughout the euphotic zone for each sampling date. Incident PAR was obtained from the NERRS Taskinas Creek station, located 45 km from the VCU RRC pier. Irradiance (I) at each 0.5 m depth (z) interval was derived based on incident PAR (I_o) during incubation, the light

attenuation coefficient (K_d; m^{-1}) and depth (Wetzel 1975, Hambrook-Berkman and Canova 2007; Equation 5).

$$I_z = I_o e^{-K_d z} \qquad (5)$$

The light attenuation coefficient was derived from the regression of the log transformed down-welling irradiance versus depth (Kirk 1994). Vertical light attenuation profiles were measured in quadruplicate at 0.5 m intervals using a LI-COR model LI-1400 data logger equipped with underwater and surface quantum sensors. Chlorophyll-a (CHLa) samples were collected during each incubation to derive biomass-specific rates of production. Samples for pigment analysis were filtered through Whatman GF/A glass fiber filters, extracted in a 90% buffered acetone solution for 18 hours and analyzed on a Turner Design TD-700 Fluorometer (Sellers and Bukaveckas 2003, Bukaveckas et al. 2011).

Statistics

For the VECOS dataset, a three-way analysis of variance (ANOVA) was performed using segment, method, month, and their interaction terms to explain variation in monthly mean GPP and ER. For the Rice Pier dataset, a two-way ANOVA was utilized with month, method, and their interaction term as independent variables. Linear regressions were performed to assess relationships between monthly mean GPP and ER with environmental variables (i.e., monthly mean water temperature and CHLa concentration). Independent sample t-tests were used to compare means and to determine statistical significance ($p < 0.05$) across metabolic estimates derived using either Caffrey or Bayesian methods. Days with negative GPP values constituted < 5% of all daily estimates and were not removed from statistical analysis. All Bayesian analyses, multiple regressions, two and three way ANOVA's were derived using Rstudio (R Core Team 2017). Caffrey estimates were derived using a metabolism program written in Matlab.

Independent sample t-tests were performed using SPSS and path-analysis (see appendix) were derived using AMOS (IBM Corp. Version 23.0).

Results

Analysis of 2006-2008 VECOS Data

For the longitudinal (VECOS) time series, three-way ANOVA results showed that longitude (salinity segments) accounted for the greatest proportion of variation in both GPP and ER (46 and 56%, respectively; Fig. 3 and Table 3). Month accounted for the second largest proportion of variation in GPP and ER (22 and 14%, respectively). Method was also a significant factor but its effects on GPP and ER varied by segment and month as indicated by significant interaction effects. This was further supported by the greater coefficient of variation for $GPP_{Caffrey}$ and $ER_{Caffrey}$ estimates for each segment across months and years, indicating lower variation in Bayesian derived metabolic estimates (Table 4). Monthly average $GPP_{Caffrey}$ and $ER_{Caffrey}$ varied 5-fold throughout the JRE, with $AE_{Caffrey}$ accounting for a small proportion of O_2 fluxes (14% of $ER_{Caffrey}$ and 24% of $GPP_{Caffrey}$). $GPP_{Bayesian}$ and $ER_{Bayesian}$ had less variation than Caffrey estimates, varying 2-fold throughout the estuary, with $AE_{Bayesian}$ accounting for 10% of $ER_{Bayesian}$ and 12% of $GPP_{Bayesian}$. Both methods indicated that the lower TF segment was net autotrophic (mean $NEM_{Caffrey} = 1.43 \pm 0.25$, mean $NEM_{Bayesian} = 0.93 \pm 0.60$ g O_2 m^{-2} d^{-1}) between spring and fall, with average net heterotrophy in all other segments. Overall, 87% of the total variation in GPP and 92% of the total variation ER was explained, with longitudinal differences accounting the greatest amount of variation, followed by monthly variation and methodological differences.

Both methods agreed on the rank order of GPP and ER among segments, with greatest rates in the polyhaline (mean $GPP_{Caffrey} = 20.71 \pm 1.43$, mean $ER_{Caffrey} = 22.07 \pm 1.33$, mean

$GPP_{Bayesian}$ = 13.39 ± 0.62, mean $ER_{Bayesian}$ = 16.4 ± 0.28 g O_2 m^{-2} d^{-1}) and lowest rates in the upper TF (mean $GPP_{Caffrey}$ = 3.84 ± 0.66, mean $ER_{Caffrey}$ = 4.86 ± 0.62, mean $GPP_{Bayesian}$ = 6.46 ± 0.38, mean $ER_{Bayesian}$ = 10.47 ± 0.31 g O_2 m^{-2} d^{-1}; Fig. 4). $GPP_{Bayesian}$ estimates were greater than $GPP_{Caffrey}$ in the upper TF segment, while $GPP_{Caffrey}$ was greater than $GPP_{Bayesian}$ in the polyhaline segment (R^2 = 0.83, $p < 0.001$). This pattern was consistent for ER, with $ER_{Bayesian}$ exceeding $ER_{Caffrey}$ in the upper TF and $ER_{Caffrey}$ exceeding $ER_{Bayesian}$ in the polyhaline (R^2 = 0.68, $p < 0.001$). The two methods yielded similar estimates of AE which were highly correlated (R^2 = 0.97, $p < 0.001$, m = 1.05). AE in the lower TF segment was persistently negative for both methods indicating that this segment had a net flux of O_2 out of the water column.

In order to determine the sources of OM (i.e., autochthonous or allochthonous) supporting metabolism throughout the estuary, the y-intercept of the ER vs. GPP linear regression was interpreted as the proportion of ER supported by allochthonous sources (i.e., ER when GPP = 0; del Giorgio and Peters 1994; Fig. 5). For the Caffrey estimates, allochthonous ER was 0.58 ± 0.02 g O_2 m^{-2} d^{-1}, while average $ER_{Caffrey}$ was 12.49 ± 0.71 g O_2 m^{-2} d^{-1} indicating that 95% of ER was supported by autochthonous OM sources (e.g., algal production). For Bayesian estimates, allochthonous ER was 7.71 ± 0.07 g O_2 m^{-2} d^{-1}, while average $ER_{Bayesian}$ was 12.99 ± 0.28 g O_2 m^{-2} d^{-1} indicating that ER was primarily supported by allochthonous OM sources (e.g., sediments). Thus an important difference between the two methods is that the Caffrey results indicate that metabolism was supported by autochthonous sources, whereas the Bayesian method indicates that metabolism is supported by allochthonous OM subsidies.

Analysis of 2009-2016 Rice Pier Data

Annual $NEM_{Caffrey}$ was net autotrophic from 2010-2014, approximately equal in 2016 and net heterotrophic in 2009 and 2015 (Fig. 6). On average, $GPP_{Caffrey}$ exceeded $ER_{Caffrey}$ by 0.43 ±

0.19 g O_2 m^{-2} d^{-1} over the 8-year span. $GPP_{Caffrey}$ and $ER_{Caffrey}$ followed seasonal trends in PAR and water temperature with highest rates (GPP = 10.90 ± 0.53, ER = 10.12 ± 0.40 g O_2 m^{-2} d^{-1}) during June-September and lowest rates (GPP = 1.40 ± 0.18, ER = 2.04 ± 0.19 g O_2 m^{-2} d^{-1}) during December-February. Results from the Bayesian analysis differed from the Caffrey metabolism estimates in that they yielded higher ER and therefore lower NEM (Fig. 6). $GPP_{Bayesian}$ displayed similar seasonal patterns to $GPP_{Caffrey}$ with greatest rates during summer (mean = 12.18 ± 0.46 g O_2 m^{-2} d^{-1}) and lowest rates in winter (mean = 3.95 ± 0.16 g O_2 m^{-2} d^{-1}; Fig. 6b). However, $ER_{Bayesian}$ showed low seasonal variation (summer = 8.82 ± 0.59 g O_2 m^{-2} d^{-1}, winter = 7.75 ± 0.31 g O_2 m^{-2} d^{-1}) and was not well correlated with $GPP_{Bayesian}$ (R^2 = 0.12, p = 0.001). With less seasonality, $ER_{Bayesian}$ was overall higher and exceeded $GPP_{Bayesian}$ by 0.42 ± 0.36 g O_2 m^{-2} d^{-1}. Thus an important difference between the two methods of estimating metabolism is that the Caffrey results indicated net autotrophic conditions (GPP > ER), whereas the Bayesian method indicated net heterotrophic conditions (ER > GPP).

For the 8-year time series, a two-way ANOVA showed that both month and methodology accounted for a significant proportion of variation in GPP (R^2 = 0.76, p < 0.001). There was no significant interaction between the model factors indicating that the effect of methodology was consistent across months. This was further supported by the strong correlation between the two sets of GPP estimates (R^2 = 0.93, p < 0.001; Fig. 7). When GPP was in the upper half of its range (8-16 g O_2 m^{-2} d^{-1}) $GPP_{Caffrey}$ was greater than $GPP_{Bayesian}$, whereas when GPP was lower (< 8 g O_2 m^{-2} d^{-1}) $GPP_{Bayesian}$ was greater than $GPP_{Caffrey}$. Daily average $GPP_{Bayesian}$ (mean = 7.89 ± 0.36 g O_2 m^{-2} d^{-1}) was 25% higher than $GPP_{Caffrey}$ (6.29 ± 0.45 g O_2 m^{-2} d^{-1}). The two-way ANOVA included a significant interaction effect for ER, indicating that differences between the two methods were not consistent across months (R^2 = 0.68, p < 0.001). $ER_{Caffrey}$ ranged 5-fold

between summer (mean = 10.12 ± 0.4 g O_2 m^{-2} d^{-1}) and winter (mean = 2.04 ± 0.19 g O_2 m^{-2} d^{-1}), whereas summer $ER_{Bayesian}$ (mean = 9.28 ± 0.53 g O_2 m^{-2} d^{-1}) was only 20% greater than winter $ER_{Bayesain}$ (mean = 7.75 ± 0.31 g O_2 m^{-2} d^{-1}). $ER_{Bayesian}$ estimates were greater than $ER_{Caffrey}$ when ER was in the lower half (< 8 g O_2 m^{-2} d^{-1}) of its range (R^2 = 0.21, $p < 0.001$). Daily average $ER_{Bayesian}$ was 41% higher (mean = 8.31 ± 0.24 g O_2 m^{-2} d^{-1}) than $ER_{Caffrey}$ (mean = 5.86 ± 0.38 g O_2 m^{-2} d^{-1}, $p < 0.001$). The two methods yielded similar estimates of AE which were strongly correlated (R^2 = 0.98, $p < 0.001$, m = 1.22) however, $AE_{Bayesian}$ had higher maximum and lower minimum estimates than $AE_{Caffrey}$. Using an independent sample t-test, AE estimates using both methods were not significantly different from each other ($AE_{Bayesian}$ = -1.02 ± 0.16 g O_2 m^{-2} d^{-1}; $AE_{Caffrey}$ = -0.71 ± 0.13 g O_2 m^{-2} d^{-1}, $p = 0.144$). AE was on average negative, indicating persistent O_2 supersaturation in the water column with a net flux of O_2 into the atmosphere.

$GPP_{Caffrey}$ and $ER_{Caffrey}$ were highly correlated (R^2 = 0.83, $p < 0.001$) whereas $GPP_{Bayesian}$ and $ER_{Bayesian}$ were weakly correlated (R^2 = 0.12, $p < 0.001$; Fig. 8). Caffrey results showed that allochthonous ER was 1.01 ± 0.03 g O_2 m^{-2} d^{-1}, while average $ER_{Caffrey}$ was 5.86 ± 0.38 g O_2 m^{-2} d^{-1} indicating that 83% of $ER_{Caffrey}$ was supported by autochthonous OM production. For Bayesian estimates, allochthonous ER was 6.51 ± 0.06 g O_2 m^{-2} d^{-1}, while average $ER_{Bayesian}$ was 8.31 ± 0.24 g O_2 m^{-2} d^{-1} indicating that $ER_{Bayesian}$ was predominantly supported by allochthonous OM. Caffrey results indicate that metabolism was supported by autochthonous production, whereas the Bayesian results indicate that metabolism was supported by allochthonous OM subsidies.

The proportion of ecosystem metabolism contributed by pelagic GPP or R was determined using both Caffrey and Bayesian estimates. Pelagic metabolism accounted for a similar proportion of $GPP_{Caffrey}$ and $ER_{Caffrey}$ in comparison to the corresponding Bayesian values

(Fig. 9). Pelagic GPP (mean = 6.11 ± 0.66 g O_2 m^{-2} d^{-1}) accounted for on average 65% of $GPP_{Caffrey}$ (mean = 9.45 ± 1.20 g O_2 m^{-2} d^{-1}) and 57% of $GPP_{Bayesian}$ (mean = 10.68 ± 0.93 g O_2 m^{-2} d^{-1}). Pelagic R (3.28 ± 0.42 g O_2 m^{-2} d^{-1}) accounted for 37% of $ER_{Caffrey}$ (8.71 ± 1.04 g O_2 m^{-2} d^{-1}) and 28% of $ER_{Bayesian}$ (11.79 ± 0.99 g O_2 m^{-2} d^{-1}). Pelagic GPP and R were found to be more strongly correlated with the Caffrey estimates (R^2 = 0.73 and 0.62, respectively) than with the corresponding Bayesian values (R^2 = 0.63 and 0.15).

Water temperature and CHLa were strongly related to $GPP_{Bayesian}$, $GPP_{Caffrey}$ and $ER_{Caffrey}$, while only water temperature was related to $ER_{Bayesian}$ estimates (Fig. 10). Using a multiple linear regression, water temperature accounted for 84% of the variation in $GPP_{Caffrey}$ and 85% in $GPP_{Bayesian}$, with CHLa accounting for an additional 2% and 1% of variation in both $GPP_{Caffrey}$ and $GPP_{Bayesian}$ respectively ($GPP_{Caffrey}$ R^2 = 0.86, $p < 0.001$ and $GPP_{Bayesian}$ R^2 = 0.86, $p < 0.001$). Water temperature also had a positive linear relationship with $ER_{Caffrey}$ estimates (R^2 = 0.80, $p < 0.001$), with CHLa accounting for an additional 2% of $ER_{Caffrey}$. Water temperature was weakly correlated with $ER_{Bayesian}$ estimates (R^2 = 0.21, $p < 0.001$). Water temperature and CHLa showed similar strong correlations with $GPP_{Bayesian}$, $GPP_{Caffrey}$ and $ER_{Caffrey}$ estimates (R^2 = 0.86, 0.86 and 0.82 respectively), while $ER_{Bayesian}$ had a weak correlation with water temperature (R^2 = 0.21).

Bayesian Scenario Comparison

The three modeling scenarios generally yielded similar estimates of ecosystem GPP, ER and AE to those obtained from the original Bayesian model (Table 5). Daily average $GPP_{Bayesian}$ for the 8-year time series was 7.9 ± 0.1 g O_2 m^{-2} d^{-1} but ranged between 8.1 ± 0.1, 7.8 ± 0.1 and 7.3 ± 0.1 g O_2 m^{-2} d^{-1} among the 3 scenarios (AB1, AB2 and AB3 respectfully). $GPP_{Bayesian}$ derived using the generic $GPP_{Bayesian}$ prior (AB3) were significantly lower than those derived

using estuarine-specific priors, though the proportional difference was small (8%, $p < 0.001$, Fig. 11a). Daily average $ER_{Bayesian}$ was 8.3 ± 0.1 g O_2 m^{-2} d^{-1} but ranged from 8.4 ± 0.1, 9.4 ± 0.1 and 7.6 ± 0.04 g O_2 m^{-2} d^{-1} among scenarios AB1, AB2 and AB3 (respectfully). Statistically significant effects were observed when estuarine-specific priors were replaced with a generic $ER_{Bayesian}$ prior (AB3), which yielded estimates 8% lower than the original model, and, when using a generic atmospheric exchange value (AB2), which yielded estimates 13% higher than the original model ($p < 0.001$, Fig. 11b). For all Bayesian model scenarios, estimates of atmospheric exchange were small (≤ 1 g O_2 m^{-2} d^{-1}) in comparison to $GPP_{Bayesian}$ and $ER_{Bayesian}$ (~8 g O_2 m^{-2} d^{-1}). Due to low rates of AE, proportional differences among the 4 scenarios were larger, but absolute differences were small, ranging from -0.3 ± 0.1 g O_2 m^{-2} d^{-1} to -1.0 ± 0.04 g O_2 m^{-2} d^{-1}. The use of fixed depth (AB1) and generic exchange coefficients (AB2) yielded significantly lower rates of atmospheric exchange ($p < 0.001$, Fig. 11c). Overall, these results show that for an 8-year time series of data, assumptions about priors and the effects of tidal variation in depth had statistically detectable effects on estimates of $GPP_{Bayesian}$, $ER_{Bayesian}$ and $AE_{Bayesian}$, but that differences among the scenarios were small (< 10%) in comparison to seasonal and inter-annual variation.

Discussion

Methodological Variation in Metabolism

Seasonal, inter-annual and longitudinal rates of ecosystem metabolism were sensitive to the method used to derive them. Temperature is a ubiquitous predictor of metabolic rates in estuaries (Caffrey 2004, Hoellein et al. 2013, Testa et al. 2012), however monthly average $ER_{Bayesian}$ had a weak relationship ($R^2 = 0.21$) with water temperature compared to $ER_{Caffrey}$ ($R^2 = 0.80$). Seasonal variation in $ER_{Bayesian}$ was low with average winter $ER_{Bayesian}$ being 20% lower

than summer rates compared to $ER_{Caffrey}$ that had a 5-fold difference between winter and summer. Low seasonality in ER of temperate estuaries is uncommon and lead to a negative 8-year average $NEM_{Bayesian}$ (-0.42 ± 0.36 g O_2 m^{-2} d^{-1}) indicating net heterotrophic conditions, whereas $NEM_{Caffrey}$ produced net autotrophic (0.43 ± 0.19 g O_2 m^{-2} d^{-1}) conditions which is consistent with prior metabolic work in this system (Smith and Kemp 1995, Caffrey 2004, Bukaveckas et al. 2011, Yvon-Durocher et al. 2012). Longitudinal rates of GPP, ER and AE were well correlated across methods (R^2 = 0.83, 0.68 and 0.97 respectively), however Bayesian estimates consistently had lower maximums and higher minimums than Caffrey estimates. Estuarine ER and GPP are typically well correlated (Caffrey 2004, Hoellein et al. 2013) which was supported by Caffrey estimates (R^2 = 0.96) across all salinity segments but was inconsistent with Bayesian estimates (R^2 = 0.35). Differences in the correlation between ER and GPP exposed another important distinction between the methods, that $ER_{Caffrey}$ was driven by autochthonous OM whereas $ER_{Bayesain}$ was mainly driven by allochthonous OM. Previous studies on the fate of algal production in the JRE have showed ER closely tracking GPP and that ER was mainly supported by microbial respiration of autochthonous OM (Bukaveckas et al. 2011, Wood et al. 2016). Thus determining which method to use when deriving metabolic estimates is important as it can impact our perception of the trophic status (i.e., CO_2 sink or source) and OM sources supporting an estuary.

Similar to Holtgrieve et al. (2010), $AE_{Bayesian}$ estimates were sensitive to the reaeration coefficient (k_{600}) used and as we show, to variation in depth by tidal influences on water surface elevation. When estuarine-specific priors (0.39 ± 0.23 d^{-1}) for daily reaeration were applied to the Bayesian model, daily average $AE_{Bayesian}$ over 8-years was 3-fold greater than when generic (stream-specific) priors (1.79 ± 1 d^{-1}) were used. Holtgrieve et al. (2010) showed how increasing

reaeration coefficient priors can significantly dampen model derived dissolved oxygen concentration in a stream. Furthermore, when tidal variation in depth was included in the Bayesian model rather than using a fixed depth, daily average $AE_{Bayesian}$ was 2-fold greater. Thus, future metabolic estimates using Bayesian methods to model AE should use site-specific reaeration coefficients and include tidal effects on local depth as AE estimates in estuaries are sensitive to changes in these model input parameters.

Longitudinal Metabolism

Rates of GPP and ER increased longitudinally between the freshwater and saline sites of the James River Estuary. Between the salinity end-members (i.e., upper TF and polyhaline segments) $GPP_{Caffrey}$ and $ER_{Caffrey}$ increased 5-fold while $GPP_{Bayesian}$ and $ER_{Bayesian}$ increased 2-fold, which is comparable to what others have found in estuaries, which can have metabolic rates vary up to 10-fold between segments (Cloern et al. 2014). All segments except the lower TF were net heterotrophic (ER > GPP) and on the whole, the JRE is annually net heterotrophic (area weighted $NEM_{Caffrey} = -0.57 \pm 0.45$ g O_2 m^{-2} d^{-1} and $NEM_{Bayesian} = -2.15 \pm 0.89$ g O_2 m^{-2} d^{-1}) which is within range for Mid-Atlantic estuaries (Caffrey 2004) and consistent with Hoellein et al. (2013) who described 89% of estuaries as net heterotrophic. No distinct difference was observed in the degree of heterotrophy between the upper TF and polyhaline segments (using either method) due to proportional increases in both GPP and ER, which is in contrast to other estuaries that have observed greater heterotrophy at small (by area), low salinity sites (Kemp et al. 1997, Raymond et al. 2000, Caffrey 2004, Tomaso and Najjar 2015). Greater heterotrophy at low salinity sites could occur when high allochthonous loads impede production (by increasing turbidity) and stimulate microbial decomposition (Gazeau et al. 2005). Since there is no significant difference in NEM between our salinity end-members ($p = 0.154$), these results

suggest rapid nutrient cycling between respired OM and primary production at the salinity end-members.

Atmospheric exchange throughout the estuary was a small component (≤ 24%) of biologically driven fluxes in O_2. AE was persistently negative in the lower TF segment using either method, indicating that this segment of the estuary had a net flux of O_2 out of the water column and was thus a CO_2 sink which is consistent with earlier findings from the tidal freshwater JRE (Bukaveckas et al. 2011). Similarly, the oligohaline segment experienced a net flux of O_2 out of the water column (negative AE) between March-June before becoming heterotrophic from July-October. All other segments were net sinks for O_2 and were thus CO_2 sources. Longitudinally, $AE_{Bayesian}$ estimates were routinely less than $AE_{Caffrey}$ estimates and similar to Holtgrieve et al. (2010). $AE_{Bayesian}$ estimates were highly sensitive to the reaeration coefficient used.

Inter-annual Metabolism

Rates of GPP and ER in the lower tidal fresh JRE showed similar amplitudes and timing in peak production and respiration across 8-years. These results are similar to Nesius et al. (2007) who observed similar timing (July-September) in peak production across 12-years (1989-2001) within the lower tidal freshwater JRE. Nesius et al. (2007) reported average total annual production of 230 g C m^{-2} yr^{-1} across 12-years in the lower tidal fresh segment, which is 3-fold lower than $GPP_{Caffrey}$ estimates (720 ± 35 g C m^{-2} yr^{-1}) and 4-fold lower than $GPP_{Bayesian}$ estimates (902 ± 38 g C m^{-2} yr^{-1}) assuming a photosynthetic quotient of 1.2 (O_2:CO_2 molar; Kemp et al. 1997, Caffrey 2004). Several reasons may be responsible for the large differences in total average production between this study and that of Nesius et al. (2007). Measurements derived in this study are at an ecosystem scale whereas the Nesius et al. (2007) used the ^{14}C

method which measures production within in a bottle. There also remains considerable uncertainty on the type of production the ^{14}C method measures (i.e., GPP or NPP; Cloern et al. 2014). Caffrey (2004) reported similar issues when comparing rates of production at 43 estuarine sites using the open method to studies using other methods of quantifying production. Our estimates of average annual GPP are comparable to those reported for estuaries by Caffrey (2004) which ranged between ~ 300-3300 g C m^{-2} yr^{-1}.

While ER showed greatest rates during summer months and lowest rates during winter months, mean annual $ER_{Caffrey}$ (805 ± 32 g C m^{-2} yr^{-1}) was statistically significantly less than $ER_{Bayesian}$ (1139 ± 70 g C m^{-2} yr^{-1}; $p < 0.001$) across 8-years due to low seasonality in $ER_{Bayesian}$ estimates (assuming a respiratory quotient of 1 O_2:CO_2 molar; Caffrey 2004). Elevated rates of $ER_{Bayesian}$ in winter are partially responsible for the weak correlation with $GPP_{Bayesian}$ ($R^2 = 0.12$) and suggests that high allochthonous OM processing maintains net heterotrophic conditions year-to-year. While 89% of estuaries depend on allochthonous OM to maintain heterotrophic conditions (Hoellein et al. 2013), many estuaries have a strong correlation between GPP and ER, such as the Caffrey estimates, suggesting rapid microbial decomposition of algal production (Caffrey 2004, Hopkinson and Smith 2005, Hoellein et al. 2013) and a shift to allochthonous OM during periods of low GPP. These results highlight how different methods of deriving ER can result in large differences in annualized rates of ER and sources of OM supporting ER.

Previous studies on metabolism in the tidal freshwater segment of the JRE have suggest annual net autotrophy which the Caffrey estimates supported (Bukaveckas et al. 2011, Wood et al. 2016). Hoellein et al. (2013) reported GPP (mean = 10.8 ± 6.7 g O_2 m^{-2} d^{-1}) and ER (mean = 13.6 ± 7.4 g O_2 m^{-2} d^{-1}) rates for 43 and 44 estuaries respectively, and indicates that $GPP_{Caffrey}$ (mean = 6.29 ± 0.45 g O_2 m^{-2} d^{-1}) is in the lower 27th percentile and $ER_{Caffrey}$ (mean = 5.86 ± 0.38

g O_2 m^{-2} d^{-1}) in the lower 11th percentile, suggesting that autotrophy is maintained by depressed ER and not by elevated GPP. $NEM_{Bayesian}$ indicated heterotrophy for the lower tidal fresh JRE and indicated that annual mean GPP (7.89 ± 0.36 g O_2 m^{-2} d^{-1}) and ER (8.31 ± 0.23 g O_2 m^{-2} d^{-1}) were in the lower 42nd and 23rd percentiles respectively. While both estimates agree that annual daily mean ER in this system is depressed compared to other estuaries, they suggest different trophic states of the lower tidal fresh JRE.

Intra-annual Metabolism

Monthly average $GPP_{Caffrey}$ and $ER_{Caffrey}$ were strongly related to climactic variables such as water temperature and PAR, with greatest metabolic rates in summer and lowest rates in winter, which is typical for temperate estuaries (Boynton et al. 1982, Caffrey 2004). Bayesian estimates of ER showed less seasonal variation, with $ER_{Bayesian}$ having a weak correlation to water temperature (R^2 = 0.21). Low seasonal variability in $ER_{Bayesian}$ suggest a sustained, year-round dependence on allochthonous OM which lead to maximum rates of heterotrophy in winter when $GPP_{Bayesian}$ is lowest. Caffrey estimates also developed maximum rates of heterotrophy in winter but $ER_{Caffrey}$ was strongly correlated with $GPP_{Caffrey}$ (R^2 = 0.83), suggesting a seasonal shift to increasing dependence on allochthonous OM in winter when $GPP_{Caffrey}$ reaches a seasonal minimum. Dependence on autochthonous OM could also be supported by the low ratio of total depth to photic depth in this segment of the estuary which releases phytoplankton from light limitation and leads to elevated autochthonous production throughout much of the year (Bukaveckas et al. 2011). Hopkinson and Smith (2005) observed a similar seasonal shift in OM dependence among 29 estuaries, from autochthonous OM in summer to allochthonous OM in winter, which they attributed to the seasonal variability in GPP. However, Caffrey (2004) observed summer peaks in heterotrophy in several North American estuaries, suggesting ER is

strongly related to water temperature, turbidity and timing of allochthonous OM loading. While both methods agree on the timing of peak autotrophy (i.e., summer) and heterotrophy (i.e., winter), they disagree on the dependence of allochthonous OM throughout the year.

Conclusions and Future Work

Metabolic estimates varied seasonally, inter-annually and longitudinally based on methodology. Caffrey derived metabolic estimates routinely predicted greater maximums and lower minimums than those derived using the Bayesian method. Both methods showed good agreement in estimating GPP ($R^2 = 0.93$, m = 0.78) and AE ($R^2 = 0.98$, m = 1.22), yet they differed in their ER estimates ($R^2 = 0.21$, m = 0.29). Both methods agreed on summer maximum rates of GPP and ER, but elevated $ER_{Bayesian}$ rates in winter lead to annual net heterotrophy (i.e., CO_2 source, O_2 sink) in the lower TF segment. $ER_{Caffrey}$ displayed temperature dependence with seasonal low $ER_{Caffrey}$ in winter leading to annual net autotrophy (i.e., CO_2 sink, O_2 source) in the lower TF segment. Bayesian estimates suggest that $ER_{Bayesian}$ is supported by allochthonous OM sources throughout the year whereas Caffrey estimates suggest a seasonal shift to allochthonous OM in winter when GPP is low. Average daily rates of GPP in the lower TF segment using either method are similar to other estuaries in the Mid-Atlantic but ER ranks among the lowest for North American estuaries. Between the upper TF and polyhaline segments, rates of $GPP_{Caffrey}$ and $ER_{Caffrey}$ increased 5-fold while $GPP_{Bayesian}$ and $ER_{Bayesian}$ increased 2-fold, with AE accounting for a small proportion ($\leq$ 24%) of the biological O_2 flux. All segments, with the exception of the lower TF, were heterotrophic and the degree of heterotrophy between the upper TF and polyhaline segments were not statistically different from each other due to proportional increases in both GPP and ER for both methods. Overall, both methods showed good agreement

for GPP and AE but differed in ER estimates which lead to differences in the interpretation of trophic status and the assessed importance of different sources of OM supporting ER.

Future studies of ecosystem metabolism in estuaries should consider the method used to derive metabolic estimates as this study has shown that method can impact the trophic status and the sources of OM supporting the metabolism of an estuary. While Bayesian approaches to ecosystem metabolism models offer the benefit of using site-specific prior information and propagation of model uncertainty, this study shows that Bayesian models can provide unlikely ecological patterns such as elevated ER at low temperatures. Bookkeeping approaches to ecosystem metabolism models, such as the Caffrey method are comparatively simpler than Bayesian methods as they require minimal parameterization, however they do not account for error propagation throughout the model. Further studies of ecosystem metabolism in the JRE would benefit from comparing near-shore estimates, as in this study, to study sites located off-shore as it is unknown if the JRE is laterally well-mixed. Results of this study indicate the importance of long-term and longitudinally expansive water quality data-sets as they provide a basis for understanding regional and watershed carbon dynamics.

Tables & Figures

Table 1. Site characteristics of continuous monitoring locations in the James River Estuary. Segment areas are from the Chesapeake Bay Program[1] and salinity data come from the VECOS dataset.

Segment	Salinity (ppt) mean ± SD	Segment Area (m^2)	Site Name	Distance (rkm)	Collection Years	
					VECOS	Rice Pier
Upper Tidal Fresh	0.1 ± 0.1	21,350,585	Osborne Landing	159	2006-2008	-
Lower Tidal Fresh	0.1 ± 0.1	82,161,284*	Rice Rivers Center	119	2006-2008	2009-2016
Oligohaline	2.8 ± 2.5	156,153,944**	4H Camp	71	2006-2008	-
Mesohaline	15.3 ± 4.0	331,231,113□	James River Country Club	29	2006-2008	-
Polyhaline	20.1 ± 3.0	98,094,880□□	Wythe Point	4	2006-2008	-

[1]Based on Chesapeake Bay Program segmentation scheme. Link to segmentation salinity ArcMap GIS layers can be found using the following link: https://usgs.maps.arcgis.com/home/item.html?id=d96647aad2894d2e874cb4a9189f4c4b
*Lower TF segment area included tidal fresh section of the Appomattox River.
**Oligohaline segment area included oligohaline segment of Chickahominy River.
□Mesohaline segment area included mesohaline segments of the Lafayette River and the Eastern, Southern and Western branches of the Elizabeth River.
□□Polyhaline segment area included the polyhaline segment of the Elizabeth River.

Table 2. Model specifications used in streamMetabolizer for the Bayesian analysis of the VECOS and Rice Rivers Center datasets.

Model Specifications	
Analysis	Bayesian
Algorithm	Hamiltonian Monte Carlo
Sampler	No-U-Turn Sampler (NUTS)
Chains	3
Burn-in Steps	500
Saved Steps	500
Thin Steps	1
Observation Error	0.1
Process Error	0.1
Chain Convergence Diagnostic	Gelman-Rubin ($\hat{R} = 1.0 \pm 0.1$)
Goodness-of-Fit	Linear regression (modeled v. observed DO)
Priors:	
GPP ($g\ O_2\ m^{-2}\ d^{-1}$)	10.8 ± 6.7
ER ($g\ O_2\ m^{-2}\ d^{-1}$)	-13.6 ± 7.4
k_{600} (d^{-1})	Upper TF = -0.06 ± 0.15
	Lower $TF_{VECOS} = 0.27 \pm 0.16$
	Lower $TF_{Rice} = 0.39 \pm 0.23$
	OH = -0.09 ± 0.13
	MH = 0.39 ± 0.13
	PH = 0.22 ± 0.17

Table 3. Results from three-way ANOVAs testing the effect of salinity segment (Upper TF, Lower TF, OH, MH and PH), computational method (Caffrey or Bayesian), month and the interaction of each independent variable on GPP and ER estimates from the VECOS dataset.

	GPP					ER				
Ind Variable	Df	Sum Sq	F value	p value	R^2	Df	Sum Sq	F value	p value	R^2
Segment	4	3569	149.9	< 0.001	0.46	4	4165	265.2	< 0.001	0.56
Method	1	74	12.4	< 0.001	0.01	1	14	3.6	0.058	ns
Month	8	1680	35.3	< 0.001	0.22	8	1038	33.1	< 0.001	0.14
Segment:Method	4	771	32.4	< 0.001	0.10	4	837	53.3	< 0.001	0.11
Segment:Month	26	568	3.7	< 0.001	0.07	26	230	2.3	0.001	0.03
Method:Month	8	163	3.4	0.001	0.02	8	342	10.9	< 0.001	0.05
Segment:Method:Month	26	100	0.6	0.903	ns	26	207	2.0	0.005	0.03
Residuals	148	881				148	581			
Total		7806			0.87		7414			0.92

Table 4. Inter-annual, intra-annual and longitudinal coefficients of variation (CV). Inter-annual CV was derived based on the mean and standard deviation (SD) of Caffrey or Bayesian GPP and ER for each month across all years (2006-2008) and segments. Intra-annual CV was derived based on the mean and SD of all months for each year and segment. Longitudinal CV was derived based on the mean and SD of each segment for a representative spring (April) and summer (August) month for each year.

Inter-annual Coefficient of Variation (CV) across months																				
	Upper TF				Lower TF				Oligohaline				Mesohaline				Polyhaline			
	$GPP_{Caffrey}$	$GPP_{Bayesian}$	$ER_{Caffrey}$	$ER_{Bayesian}$	$GPP_{Caffrey}$	$GPP_{Bayesian}$	$ER_{Caffrey}$	$ER_{Bayesian}$	$GPP_{Caffrey}$	$GPP_{Bayesian}$	$ER_{Caffrey}$	$ER_{Bayesian}$	$GPP_{Caffrey}$	$GPP_{Bayesian}$	$ER_{Caffrey}$	$ER_{Bayesian}$	$GPP_{Caffrey}$	$GPP_{Bayesian}$	$ER_{Caffrey}$	$ER_{Bayesian}$
March	-	-	-	-	-	-	-	-	-	-	-	-	-	-	-	-	0.28	0.14	0.15	0.11
April	0.46	0.04	0.26	0.07	0.32	0.17	0.13	0.07	0.14	0.12	0.18	0.12	0.38	0.17	0.30	0.09	0.08	0.09	0.05	0.08
May	0.58	0.07	0.38	0.09	0.17	0.14	0.12	0.09	0.18	0.07	0.17	0.08	0.05	0.05	0.06	0.02	0.23	0.13	0.19	0.05
June	0.45	0.12	0.37	0.06	0.04	0.06	0.11	0.06	0.13	0.09	0.08	0.04	0.30	0.19	0.24	0.07	0.36	0.26	0.28	0.07
July	0.48	0.18	0.38	0.09	0.03	0.04	0.07	0.09	0.09	0.08	0.11	0.06	0.15	0.17	0.09	0.05	0.06	0.03	0.06	0.02
August	0.09	0.10	0.03	0.02	0.11	0.11	0.15	0.02	0.06	0.04	0.03	0.05	0.18	0.11	0.15	0.03	0.21	0.22	0.14	0.06
September	0.84	0.30	0.57	0.10	0.29	0.27	0.18	0.10	0.20	0.09	0.12	0.07	0.09	0.05	0.13	0.10	0.25	0.12	0.27	0.05
October	0.87	0.27	0.67	0.13	0.46	0.31	0.36	0.13	0.30	0.14	0.21	0.15	0.05	0.06	0.13	0.10	0.06	0.06	0.07	0.06
November	-	-	-	-	-	-	-	-	-	-	-	-	-	-	-	-	0.25	0.17	0.16	0.07
Mean	0.54	0.16	0.38	0.08	0.20	0.16	0.16	0.08	0.16	0.09	0.13	0.08	0.17	0.11	0.16	0.07	0.20	0.14	0.15	0.06
Intra-annual CV																				
2006	0.97	0.27	0.64	0.14	0.36	0.26	0.31	0.06	0.28	0.22	0.18	0.10	0.36	0.29	0.32	0.15	0.25	0.18	0.24	0.09
2007	0.62	0.20	0.50	0.13	0.24	0.21	0.24	0.12	0.29	0.17	0.17	0.15	0.49	0.32	0.44	0.13	0.50	0.33	0.40	0.09
2008	0.80	0.33	0.63	0.15	0.33	0.22	0.24	0.08	0.22	0.22	0.08	0.12	0.43	0.29	0.38	0.11	0.32	0.22	0.30	0.10
Mean	0.80	0.27	0.59	0.14	0.31	0.23	0.26	0.09	0.26	0.20	0.14	0.12	0.43	0.30	0.38	0.13	0.36	0.24	0.32	0.09
Longitudinal CV																				
	2006				2007				2008											
April	0.63	0.32	0.61	0.24	0.68	0.31	0.71	0.30	0.78	0.33	0.71	0.20								
August	0.57	0.28	0.57	0.22	0.71	0.40	0.67	0.20	0.59	0.29	0.60	0.24								

Table 5. Daily mean ± SE of GPP, ER, AE (g O_2 m^{-2} d^{-1}) and k_{O_2} (m d^{-1}) for the lower tidal freshwater segment of the James River during 2009-2016 using the Caffrey method, Bayesian method and 3 alternative Bayesian modeling scenarios.

Method	Production	Respiration	Atm. Exchange	k_{O2}
Caffrey	6.4 ± 0.1	5.9 ± 0.1	-0.7 ± 0.03	4.8
Bayesian	7.9 ± 0.1	8.3 ± 0.1	-1.0 ± 0.04	1.5 ± 0.01
Alternative Bayesian 1 (AB1)	8.1 ± 0.1	8.4 ± 0.1	-0.5 ± 0.05	1.5 ± 0.01
Alternative Bayesian 2 (AB2)	7.8 ± 0.1	9.4 ± 0.1	-0.3 ± 0.1	7.1 ± 0.27
Alternative Bayesian 3 (AB3)	7.3 ± 0.1	7.6 ± 0.1	-0.9 ± 0.05	1.5 ± 0.01

Bayesian used site specific priors for GPP, ER and K with tidal variation in depth

AB1 used the same priors as model 1 but with a constant depth (2.5 m)

AB2 used site specific priors for GPP and ER, generic K and tidal variation in depth

AB3 used generic priors for GPP and ER, site specific K and tidal variation in depth

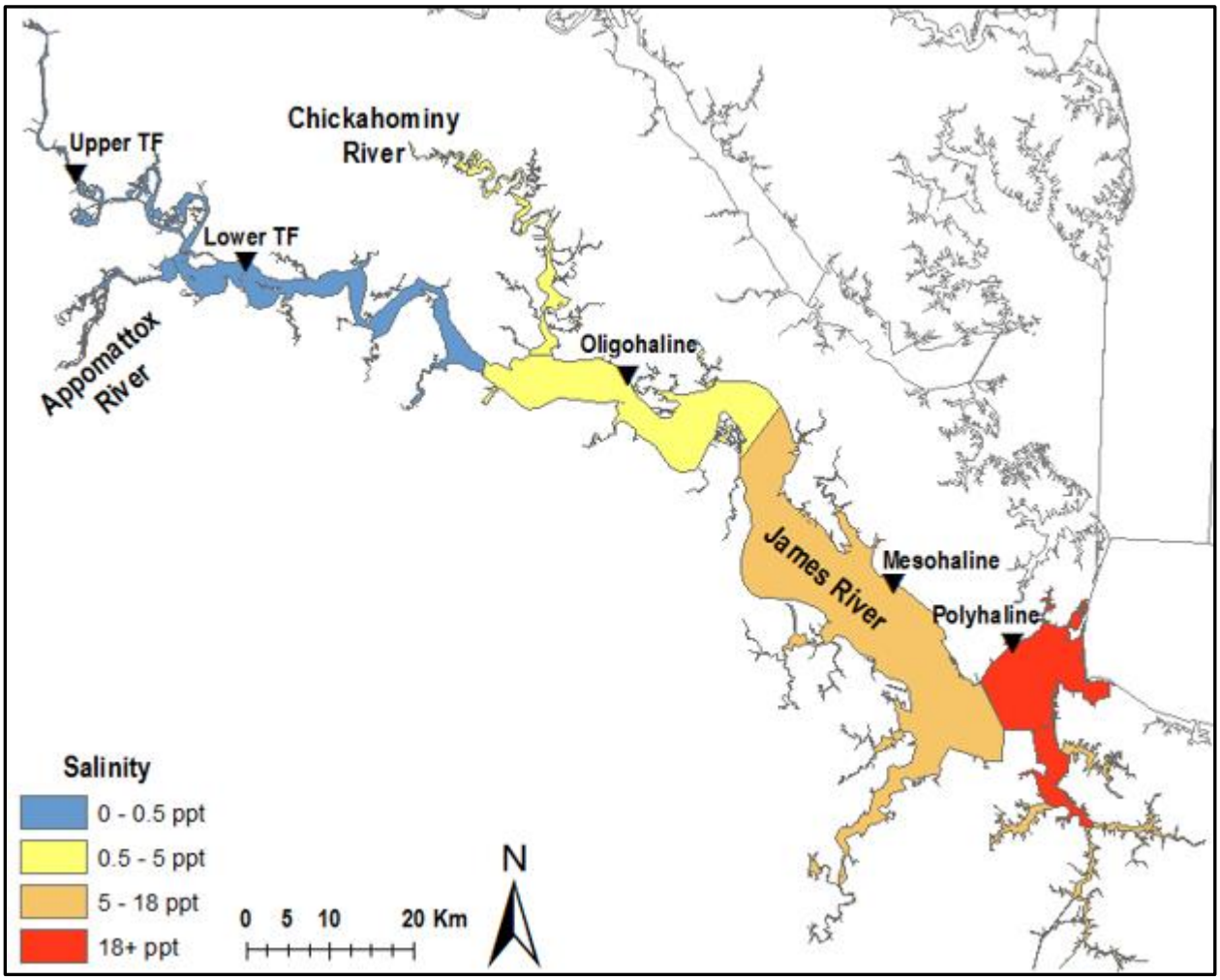

Figure 1. Salinity zones and locations of continuous monitoring sites (black triangles) within the James River Estuary.

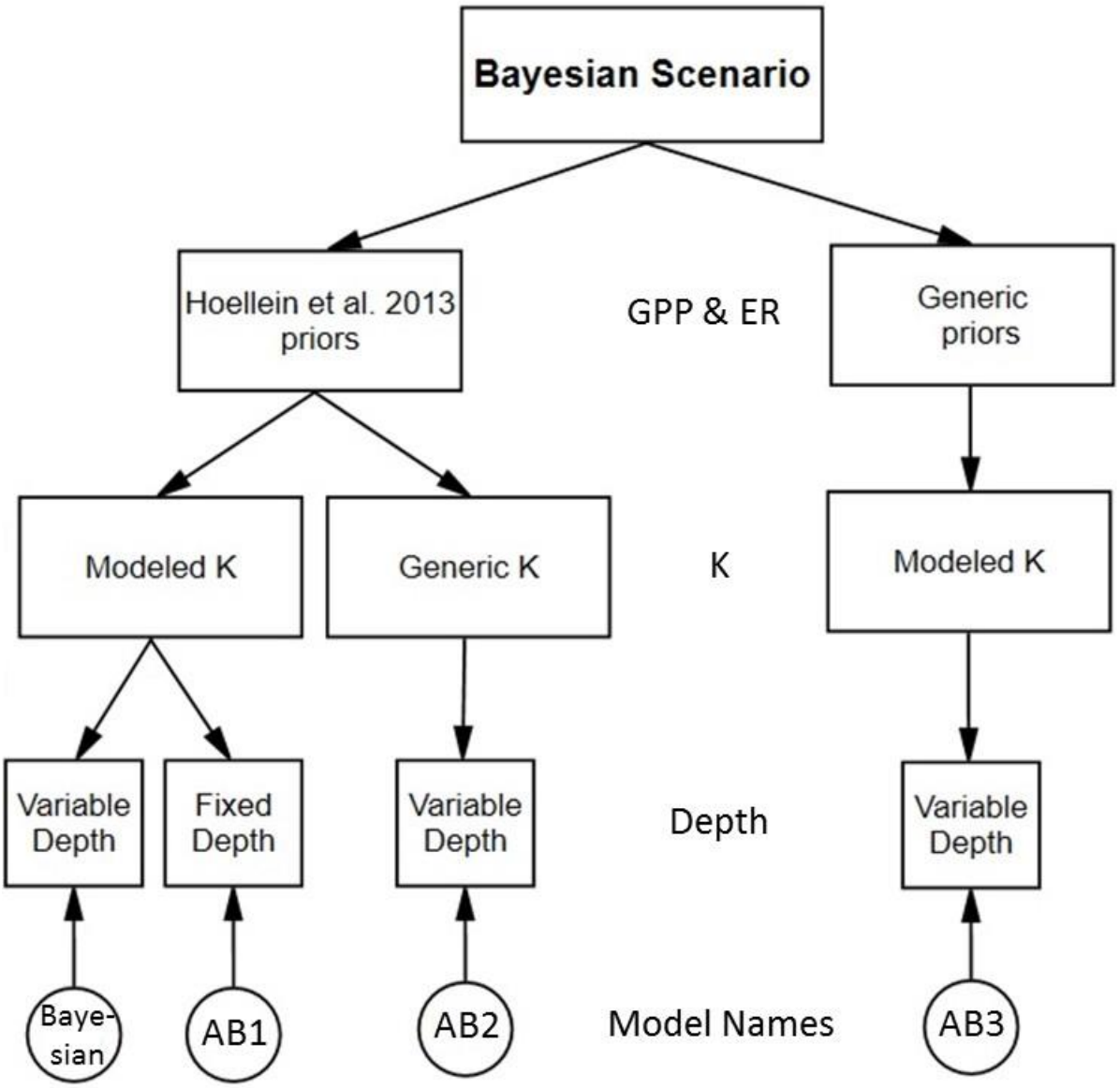

Figure 2. The Bayesian model and three alternative Bayesian modelling scenarios (AB1, AB2, AB3) were performed using Bayesian analysis to assess the sensitivity of metabolism estimates to water depth (fixed or variable) and the use of generic vs. system-specific priors for atmospheric exchange (K), GPP and ER.

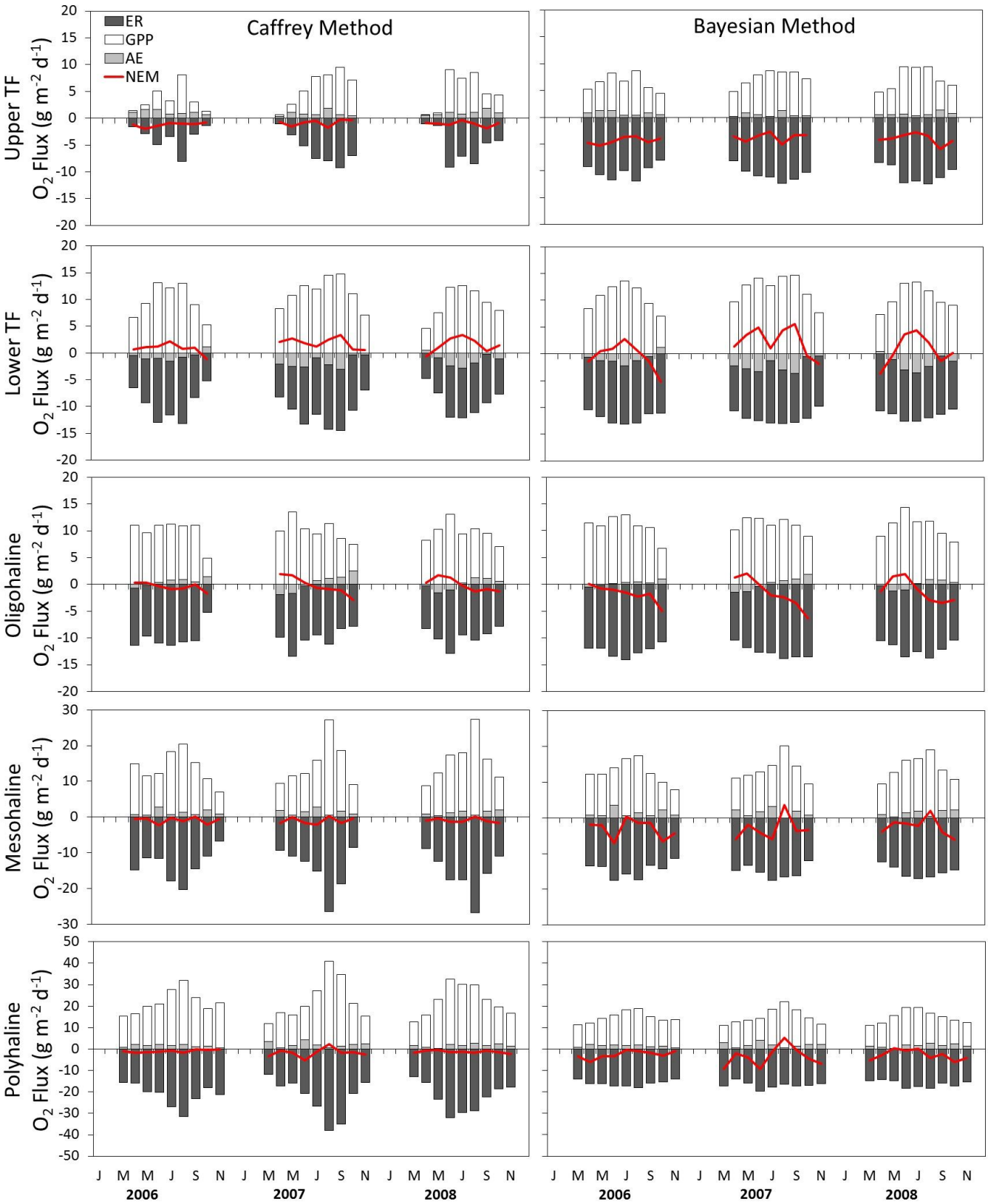

Figure 3. Monthly average GPP, ER, AE and NEM for five salinity segments of the James River Estuary derived using the Caffrey (left column) and Bayesian (right column) method.

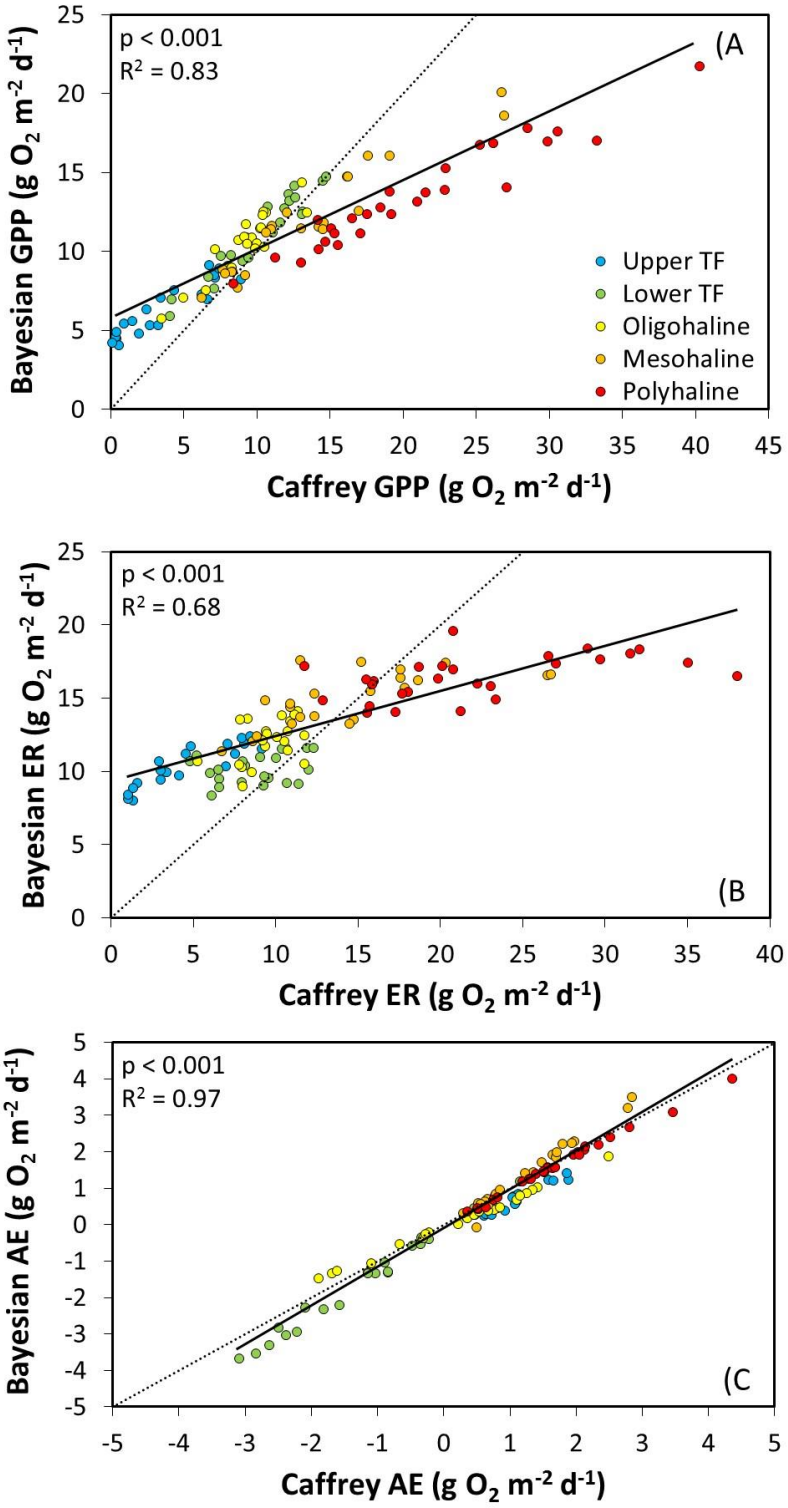

Figure 4. Comparison of Caffrey and Bayesian estimates of monthly average (A) Gross Primary Production (GPP), (B) Ecosystem Respiration (ER), and (C) atmospheric exchange (AE) among the salinity segments based on the 2006-2008 VECOS dataset. Dotted lines represent 1:1 relationship.

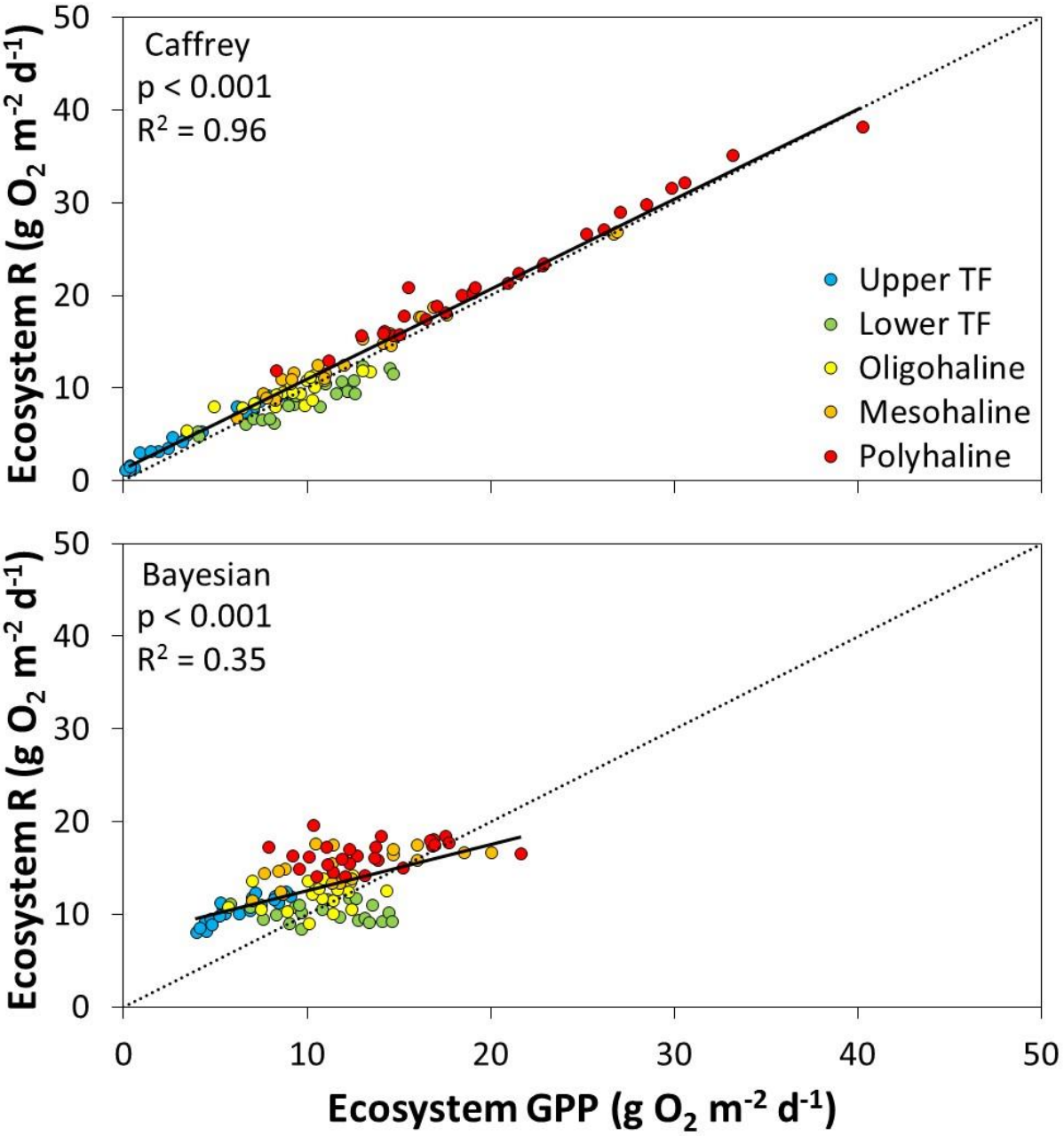

Figure 5. Linear regressions between monthly average ecosystem respiration (ER) and ecosystem GPP for each salinity segment derived using the Caffrey method (upper) and the Bayesian method (lower) from the 2006-2008 VECOS dataset. Dotted lines represent 1:1 relationship.

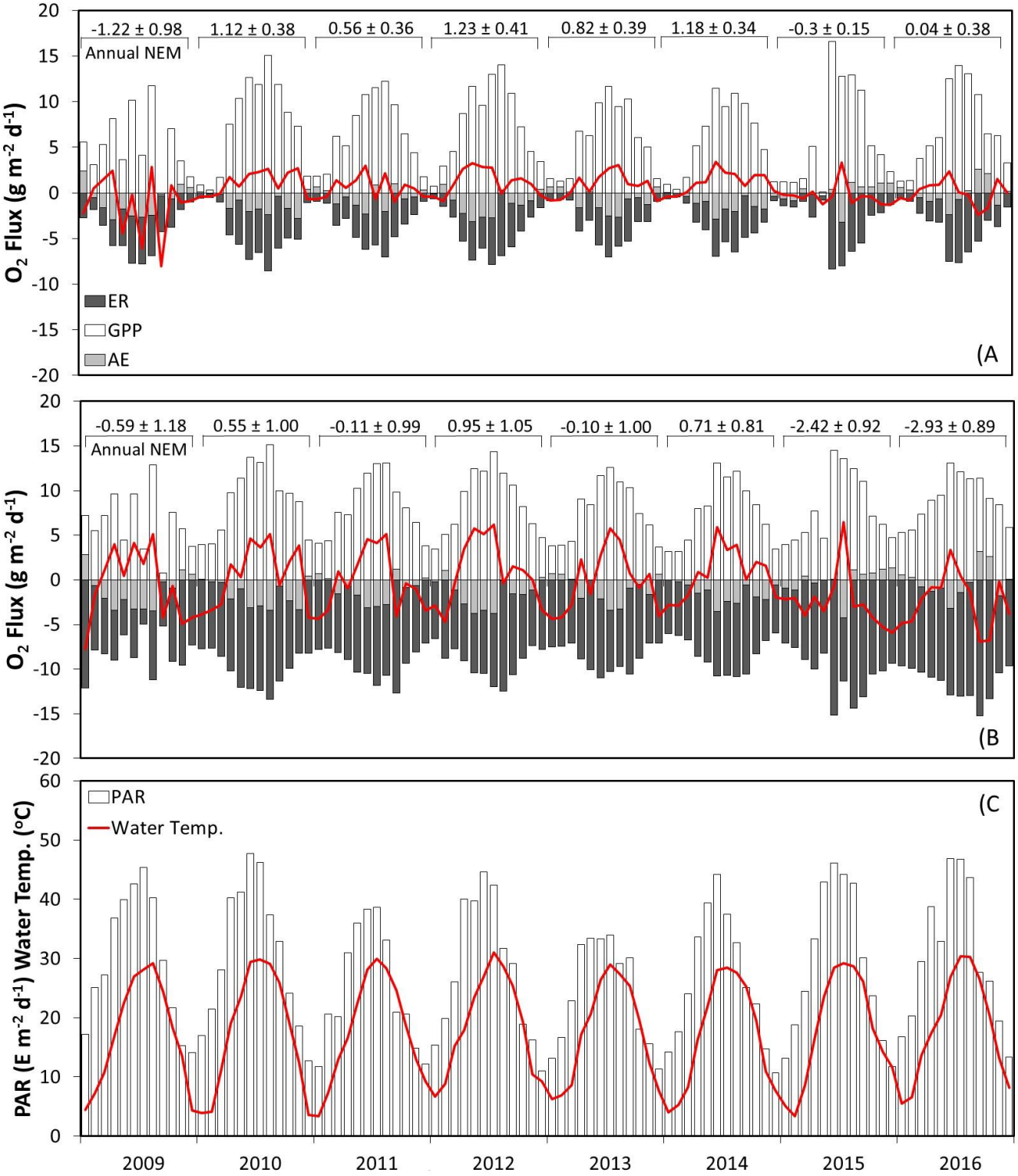

Figure 6. Monthly averages of daily ecosystem respiration (ER), gross primary production (GPP), atmospheric exchange (AE) and net ecosystem metabolism (NEM) in the lower tidal fresh segment of the James using the Caffrey method (A) and Bayesian method (B). Also shown (C), monthly mean PAR and water temperature for this station.

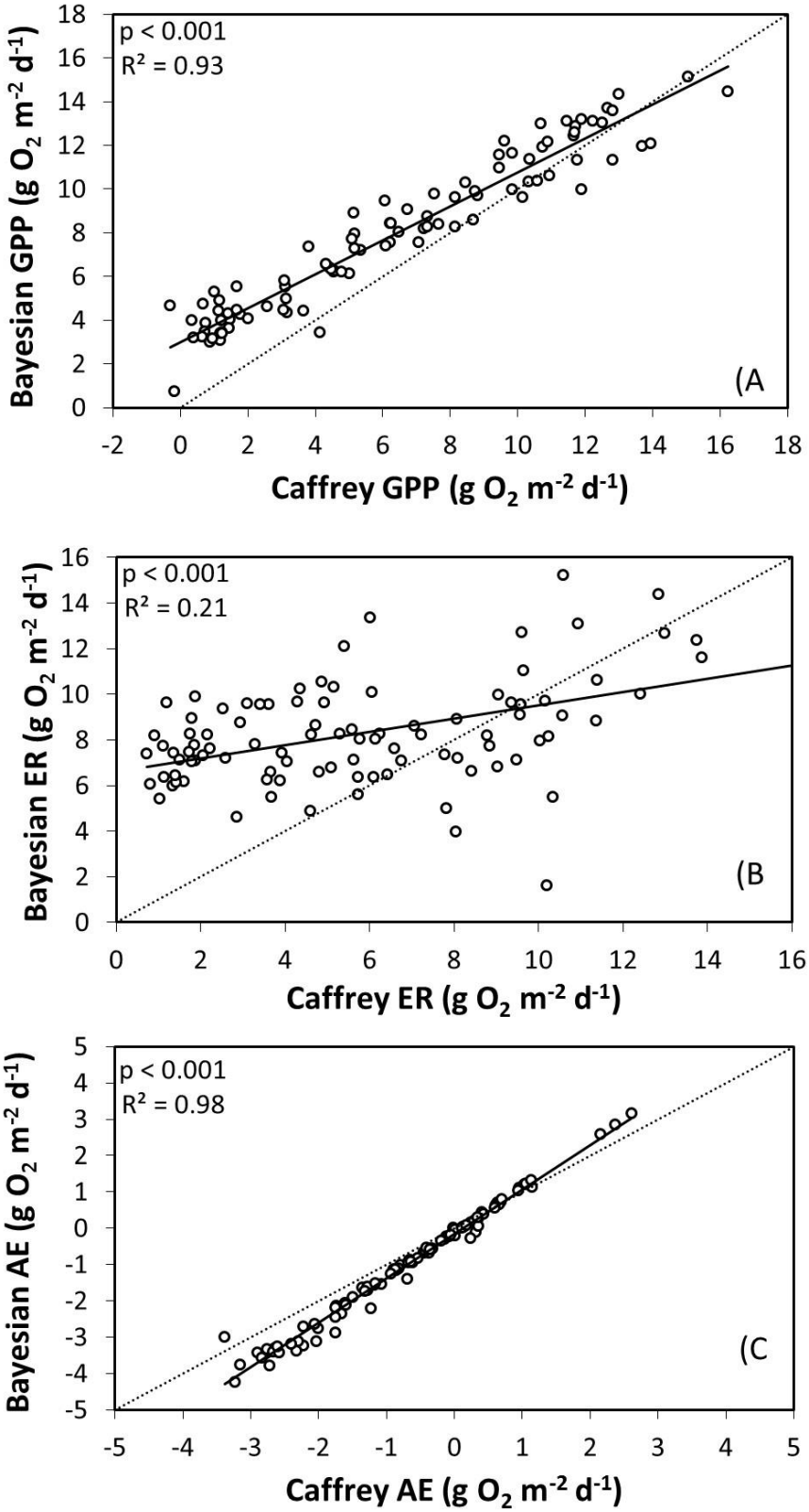

Figure 7. Comparison of Caffrey and Bayesian estimates of monthly average (A) Gross Primary Production (GPP), (B) Ecosystem Respiration (ER), and (C) Atmospheric Exchange (AE) from the 2009-2016 Rice Pier dataset. Dotted lines represent 1:1 relationship.

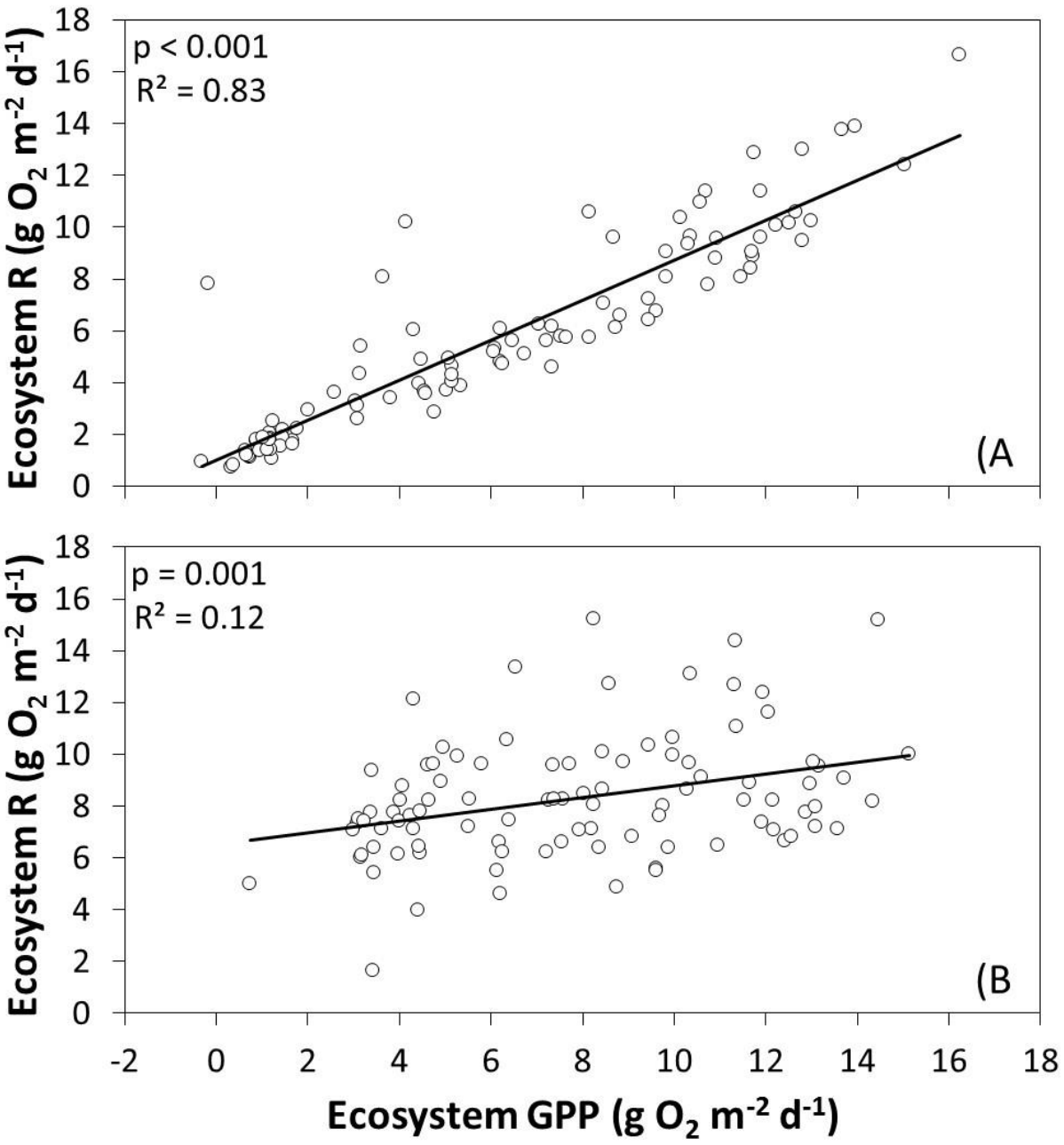

Figure 8. Linear regressions between monthly average ecosystem respiration (ER) and ecosystem GPP derived using the Caffrey method (A) and the Bayesian method (B) from the 2009-2016 Rice Pier dataset.

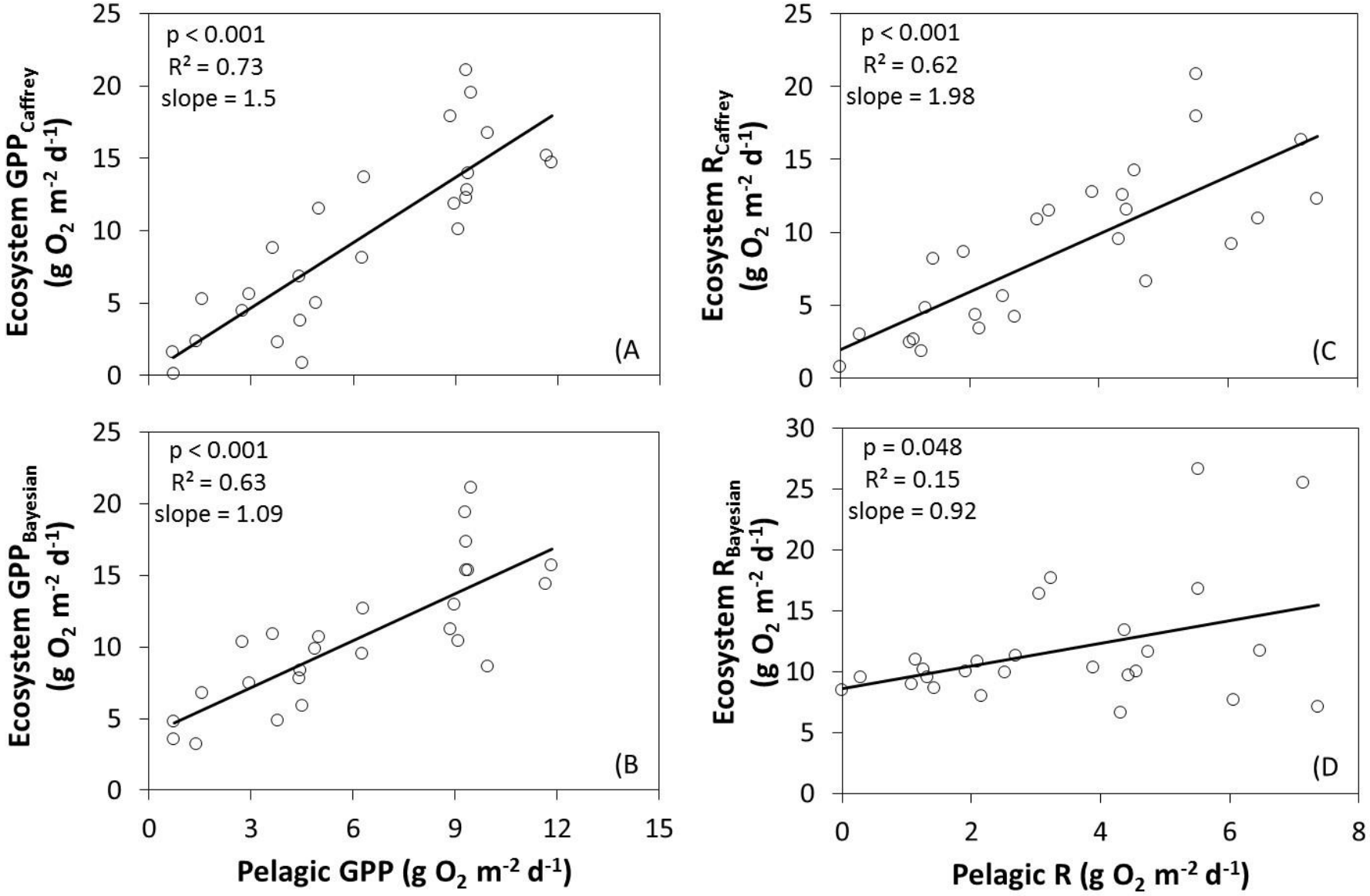

Figure 9. Pelagic metabolism as a predictor of ecosystem metabolism derived by Caffrey and Bayesian methods.

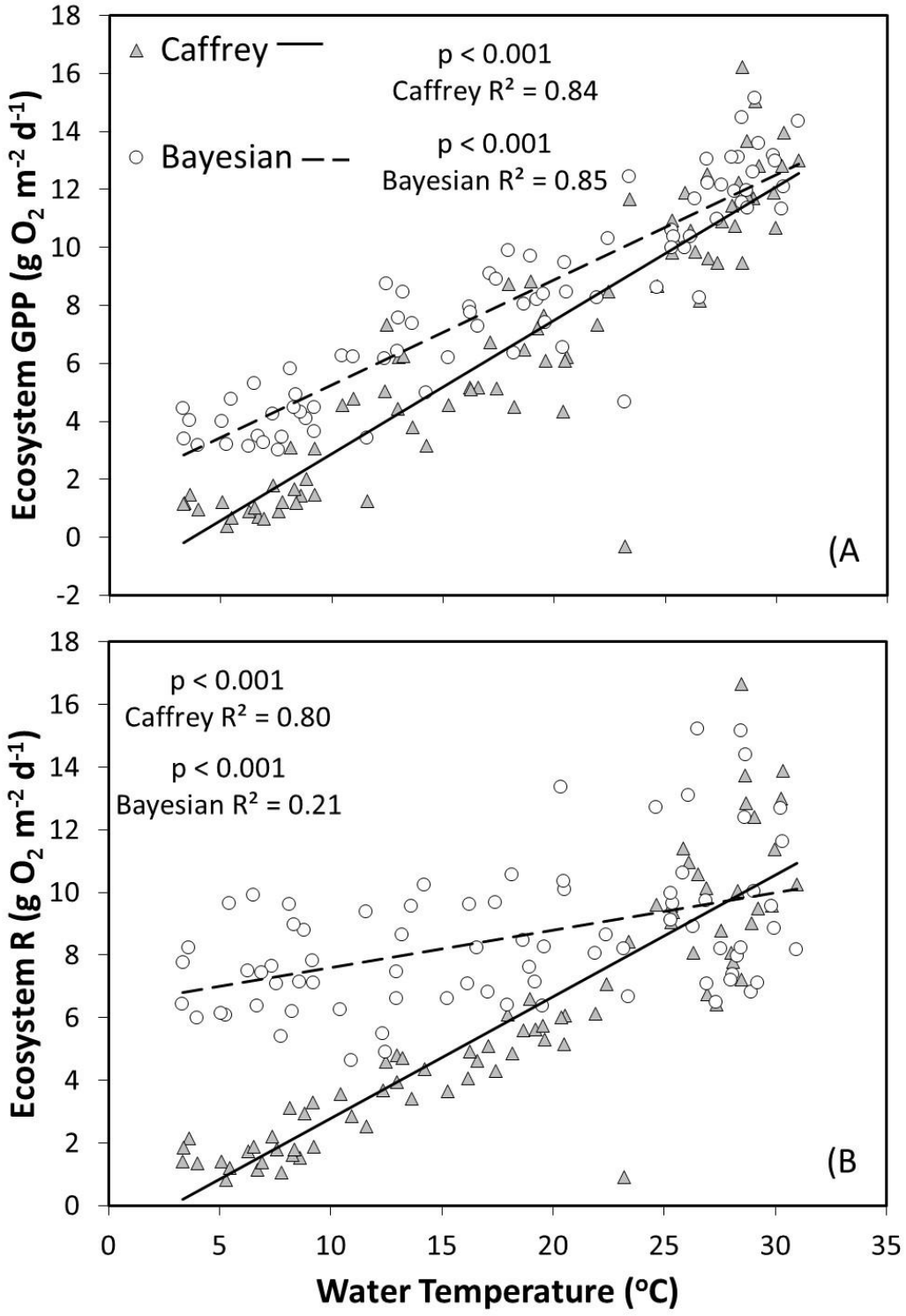

Figure 10. Monthly average GPP and ER using the Caffrey (A) and Bayesian (B) methods vs. water temperature from the lower TF segment of the JRE.

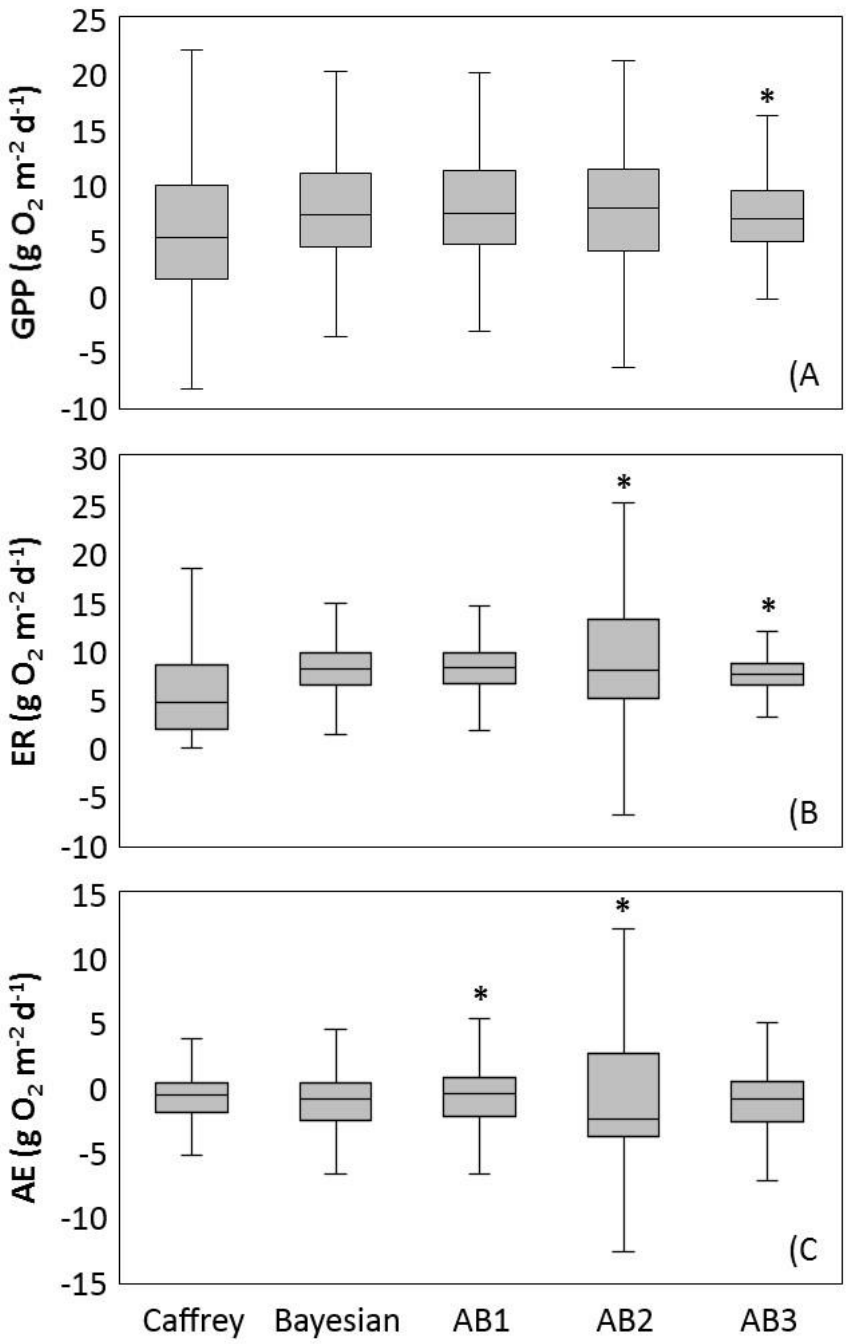

Figure 11. Daily average gross primary production (A), ecosystem respiration (B) and atmospheric exchange (C) in the James lower tidal fresh segment during 2009-2016 derived by the Caffrey method, Bayesian method and 3 alternative Bayesian (AB) modeling scenarios. The first alternative Bayesian scenario (AB1) included the same priors as the Bayesian method but with a fixed depth rather than the tidally variable depth. AB2 used generic priors for AE rather than site-specific priors. AB3 used generic GPP and ER priors rather than estuarine-specific priors. Asterisks denote a statistically significant ($p < 0.05$) difference from the Bayesian method results.

References

Alber, M., & Sheldon, J. (1999). Use of a date-specific method to examine variability in the flushing times of Georgia Estuaries. *Estuarine, Coastal and Shelf Science, 49*(4), 469-482.

Appling, A. P., Hall, R. O., Arroita, M., & Yackulic, C. B. (2017). streamMetabolizer: Models for Estimating Aquatic Photosynthesis and Respiration. R package version 0.9.33. https://github.com/USGS-R/streamMetabolizer

Borges, A. V. (2005). Do we have enough pieces of the jigsaw to integrate CO_2 fluxes in the coastal ocean? *Estuaries and Coasts, 28*(1), 3-27.

Boynton, W., Kemp, W., & Keefe, C. (1982). A comparative analysis of nutrients and other factors influencing estuarine phytoplankton production. in: Estuarine Comparisons, edited by: Kennedy, V.S., Academic Press, New York.

Bricker, S., B. Longstaff, W. Dennison, A. Jones, K. Boicourt, C. Wicks, & Woerner, J. (2007). Effects of Nutrient Enrichment in the Nation's Estuaries: A Decade of Change. NOAA CoastalOcean Program Decision Analysis Series No. 26. National Centers for Coastal Ocean Science, Silver Spring, MD. 328 pp.

Bruesewitz, D. A., Gardner, W. S., Mooney, R. F., Pollard, L., & Buskey, E. J. (2013). Estuarine ecosystem function response to flood and drought in a shallow, semiarid estuary: Nitrogen cycling and ecosystem metabolism. *Limnology and Oceanography, 58*(6), 2293-2309.

Bukaveckas, P. A., Barry, L. E., Beckwith, M. J., David, V., & Lederer, B. (2011). Factors determining the location of the chlorophyll maximum and the fate of algal production within the tidal freshwater James River. *Estuaries and Coasts, 34*(3), 569-582.

Caffrey, J. M. (2003). Production, respiration and net ecosystem metabolism in U.S. estuaries. *Environmental Monitoring and Assessment, 81*(1), 207-219.

Caffrey, J. M. (2004). Factors controlling net ecosystem metabolism in U.S. estuaries. *Estuaries and Coasts, 27*(1), 90-101.

Caffrey, J. M., Murrell, M. C., Amacker, K. S., Harper, J. W., Phipps, S., & Woodrey, M. S. (2014). Seasonal and inter-annual patterns in primary production, respiration, and net ecosystem metabolism in three estuaries in the northeast Gulf of Mexico. *Estuaries and Coasts, 37*, 222.

Carignan, R., Blais, A., & Vis, C. (1998). Measurement of primary production and community respiration in oligotrophic lakes using the Winkler method. *Canadian Journal of Fisheries and Aquatic Sciences, 55*(5), 1078-1084.

Cloern, J. E., Foster, S., & Kleckner, A. (2014). Phytoplankton primary production in the world's estuarine-coastal ecosystems. *Biogeosciences, 11*(9), 2477-2501.

Cole, J. J., Caraco, N. F., & Peierls, B. L. (1992). Can phytoplankton maintain a positive carbon balance in a turbid, freshwater, tidal estuary? *Limnology and Oceanography, 37*(8), 1608-1617.

Cole, J. J., Pace, M. L., Carpenter, S. R., & Kitchell, J. F. (2000). Persistence of net heterotrophy in lakes during nutrient addition and food web manipulations. *Limnology and Oceanography, 45*(8), 1718-1730.

Cory, R. (1974). Changes in oxygen and primary production of the Patuxent estuary, Maryland, 1963 through 1969. *Chesapeake Science, 15*(2), 78-83.

Crosswell, J. R., Wetz, M. S., Hales, B., & Paerl, H. W. (2012). Air-water CO2 fluxes in the microtidal Neuse River Estuary, North Carolina. *Journal of Geophysical Research: Oceans, 117*(C8)

D'Avanzo, C., Kremer, J. N., & Wainright, S. C. (1996). Ecosystem production and respiration in response to eutrophication in shallow temperate estuaries. *Marine Ecology Progress Series,* 263-274.

Deacon, E. (1981). Sea-air gas transfer: The wind speed dependence. *Boundary-Layer Meteorology, 21*(1), 31-37.

del Giorgio, P. A., & Peters, R. H. (1994). Patterns in planktonic P: R ratios in lakes: Influence of lake trophy and dissolved organic carbon. *Limnology and Oceanography, 39*(4), 772-787.

Fahey, T. J., & Knapp, A. K. (2007). *Principles and standards for measuring primary production* Oxford University Press.

Gazeau, F., Gattuso, J., Middelburg, J. J., Brion, N., Schiettecatte, L., Frankignoulle, M., et al. (2005). Planktonic and whole system metabolism in a nutrient-rich estuary (the Scheldt Estuary). *Estuaries and Coasts, 28*(6), 868-883.

Gelman, A., & Rubin, D. B. (1992). Inference from iterative simulation using multiple sequences. *Statistical Science,* 457-472.

Grace, M. R., Giling, D. P., Hladyz, S., Caron, V., Thompson, R. M., & Mac Nally, R. (2015). Fast processing of diel oxygen curves: Estimating stream metabolism with BASE (BAyesian Single-station estimation). *Limnology and Oceanography: Methods, 13*(3), 103-114.

Hall, R. O., Tank, J. L., Baker, M. A., Rosi-Marshall, E. J., & Hotchkiss, E. R. (2016). Metabolism, gas exchange, and carbon spiraling in rivers. *Ecosystems, 19*(1), 73.

Hall, R. O., Yackulic, C. B., Kennedy, T. A., Yard, M. D., Rosi-Marshall, E. J., Voichick, N., et al. (2015). Turbidity, light, temperature, and hydropeaking control primary productivity in the Colorado River, Grand Canyon. *Limnology and Oceanography, 60*(2), 512-526.

Hambrook-Berkman, J., & Canova, M. (2007). Algal biomass indicators. *US Geological Survey, TWRI Book, 9*

Ho, D. T., Schlosser, P., & Orton, P. M. (2011). On factors controlling air-water gas exchange in a large tidal river. *Estuaries and Coasts, 34*(6), 1103-1116.

Hobbs, N. T., & Hooten, M. B. (2015). Bayesian models: A statistical primer for ecologists Princeton University Press.

Hoellein, T. J., Bruesewitz, D. A., & Richardson, D. C. (2013). Revisiting Odum (1956): A synthesis of aquatic ecosystem metabolism. *Limnology and Oceanography, 58*(6), 2089-2100.

Hoffman, M. D., & Gelman, A. (2014). The No-U-Turn Sampler: Adaptively setting path lengths in Hamiltonian Monte Carlo. *Journal of Machine Learning Research, 15*(1), 1593-1623.

Holtgrieve, G. W., Schindler, D. E., Branch, T. A., & A'mar, Z. T. (2010). Simultaneous quantification of aquatic ecosystem metabolism and reaeration using a Bayesian statistical model of oxygen dynamics. *Limnology and Oceanography, 55*(3), 1047-1063.

Hondzo, M., Voller, V. R., Morris, M., Foufoula-Georgiou, E., Finlay, J., Ganti, V., et al. (2013). Estimating and scaling stream ecosystem metabolism along channels with heterogeneous substrate. *Ecohydrology, 6*(4), 679-688.

Hopkinson, C., & Smith, E. M. (2005). Estuarine respiration: An overview of benthic, pelagic, and whole system respiration. *Respiration in Aquatic Ecosystems,* 122-146.

Houser, J. N., Bartsch, L. A., Richardson, W. B., Rogala, J. T., & Sullivan, J. F. (2015). Ecosystem metabolism and nutrient dynamics in the main channel and backwaters of the upper Mississippi River. *Freshwater Biology, 60*(9), 1863-1879.

Hu, L., & Bentler, P. M. (1999). Cutoff criteria for fit indexes in covariance structure analysis: Conventional criteria versus new alternatives. *Structural Equation Modeling: A Multidisciplinary Journal, 6*(1), 1-55.

IBM Corp. Released 2015. IBM SPSS Statistics for Windows, Version 23.0. Armonk, NY: IBM Corp.

Jähne, B., Münnich, K. O., Bösinger, R., Dutzi, A., Huber, W., & Libner, P. (1987). On the parameters influencing air-water gas exchange. *Journal of Geophysical Research: Oceans, 92*(C2), 1937-1949.

Kemp, W., Smith, E., Marvin-DiPasquale, M., & Boynton, W. (1997). Organic carbon balance and net ecosystem metabolism in Chesapeake Bay. *Marine Ecology Progress Series*, 229-248.

Kirk, J. T. O. (1994). *Light and photosynthesis in aquatic ecosystems* Cambridge University press.

Lindeman, R. L. (1942). The trophic-dynamic aspect of ecology. *Ecology, 23*(4), 399-417.

Marino, R., & Howarth, R. W. (1993). Atmospheric oxygen exchange in the Hudson River: Dome measurements and comparison with other natural waters. *Estuaries and Coasts, 16*(3), 433-445.

Muylaert, K., Tackx, M., & Vyverman, W. (2005). Phytoplankton growth rates in the freshwater tidal reaches of the Schelde Estuary (Belgium) estimated using a simple light-limited primary production model. *Hydrobiologia, 540*(1), 127-140.

Nesius, K. K., Marshall, H. G., & Egerton, T. A. (2007). Phytoplankton productivity in the tidal regions of four Chesapeake Bay (USA) tributaries. *Virginia Journal of Science, 58*(4)

O'Connor, D., & Dobbins, W. (1958). Mechanism of reaeration in natural streams. *Transactions of the American Society of Civil Engineers*, 123, 641-684.

Odum, H. T. (1956). Primary production in flowing waters. *Limnology and Oceanography, 1*(2), 102-117.

Paerl, H. W., Rossignol, K. L., Hall, S. N., Peierls, B. L., & Wetz, M. S. (2010). Phytoplankton community indicators of short-and long-term ecological change in the anthropogenically and climatically impacted Neuse River Estuary, North Carolina, USA. *Estuaries and Coasts, 33*(2), 485-497.

R Core Team (2017). R: A language and environment for statistical computing. R Foundation for Statistical Computing, Vienna, Austria. https://www.R-project.org/.

Raymond, P. A., Bauer, J. E., & Cole, J. J. (2000). Atmospheric CO_2 evasion, dissolved inorganic carbon production, and net heterotrophy in the York River Estuary. *Limnology and Oceanography, 45*(8), 1707-1717.

Raymond, P. A., Hartmann, J., Lauerwald, R., Sobek, S., McDonald, C., Hoover, M., et al. (2013). Global carbon dioxide emissions from inland waters. *Nature, 503*(7476), 355-359.

Raymond, P. A., Zappa, C. J., Butman, D., Bott, T. L., Potter, J., Mulholland, P., et al. (2012). Scaling the gas transfer velocity and hydraulic geometry in streams and small rivers. *Limnology and Oceanography: Fluids and Environments, 2*(1), 41-53.

Roelke, D. L., Li, H., Miller-DeBoer, C. J., Gable, G. M., & Davis, S. E. (2017). Regional shifts in phytoplankton succession and primary productivity in the San Antonio bay system (USA) in response to diminished freshwater inflows. *Marine and Freshwater Research, 68*(1), 131-145.

Sellers, T., & Bukaveckas, P. A. (2003). Phytoplankton production in a large, regulated river: A modeling and mass balance assessment. *Limnology and Oceanography, 48*(4), 1476-1487.

Shen, J., Wang, Y., & Sisson, M. (2016). Development of the hydrodynamic model for long-term simulation of water quality processes of the tidal James River, Virginia. *Journal of Marine Science and Engineering, 4*(4), 82.

Smith, E. M., & Kemp, W. M. (1995). Seasonal and regional variations in plankton community production and respiration for Chesapeake Bay. *Marine Ecology Progress Series, 116*(1), 217-231.

Solomon, C. T., Bruesewitz, D. A., Richardson, D. C., Rose, K. C., Van de Bogert, Matthew C, Hanson, P. C., et al. (2013). Ecosystem respiration: Drivers of daily variability and background respiration in lakes around the globe. *Limnology and Oceanography, 58*(3), 849-866.

Testa, J. M., Kemp, W. M., Hopkinson, C. S., & Smith, S. V. (2012). Ecosystem metabolism. *Estuarine Ecology, Second Edition,* 381-416.

Thomann, R. V., & Mueller, J. A. (1987). *Principles of surface water quality modeling and control* Harper & Row, Publishers.

Tomaso, D. J., & Najjar, R. G. (2015). Long-term variations in the dissolved oxygen budget of an urbanized tidal river: The upper Delaware Estuary. *Journal of Geophysical Research Biogeosciences, 120*(6), 1027-1045.

Tranvik, L. J., Downing, J. A., Cotner, J. B., Loiselle, S. A., Striegl, R. G., Ballatore, T. J., et al. (2009). Lakes and reservoirs as regulators of carbon cycling and climate. *Limnology and Oceanography, 54*(6.2), 2298-2314.

USEPA, and Region III Chesapeake Bay Program Office. (2005). Chesapeake Bay program analytical segmentation scheme: Revisions, decisions and rationales 1983–2003, 2005 addendum. *Rep. No. EPA 903- R-05-004*, Monitoring and Analysis Subcommittee, and Tidal Monitoring and Analysis Workgroup, Annapolis, Md.

Vannote, R. L., Minshall, G. W., Cummins, K. W., Sedell, J. R., & Cushing, C. E. (1980). The river continuum concept. *Canadian Journal of Fisheries and Aquatic Sciences, 37*(1), 130-137.

Vincent, W. F., Dodson, J. J., Bertrand, N., & Frenette, J. (1996). Photosynthetic and bacterial production gradients in a larval fish nursery: The St. Lawrence River transition zone. *Marine Ecology Progress Series,* 227-238.

Wanninkhof, R. (1992). Relationship between wind speed and gas exchange over the ocean. *Journal of Geophysical Research: Oceans, 97*(C5), 7373-7382.

Wetzel, R. (1975). Limnology, *W, B. Sounders Company, Philadelphia, p.52.*

Winslow, L. A., Zwart, J. A., Batt, R. D., Dugan, H. A., Woolway, R. I., Corman, J. R., et al. (2016). LakeMetabolizer: An R package for estimating lake metabolism from free-water oxygen using diverse statistical models. *Inland Waters, 6*(4), 622-636.

Wood, J. D., & Bukaveckas, P. A. (2014). Increasing severity of phytoplankton nutrient limitation following reductions in point source inputs to the tidal freshwater segment of the James River Estuary. *Estuaries and Coasts, 37*(5), 1188.

Wood, J. D., Elliott, D., Garman, G., Hopler, D., Lee, W., McIninch, S., et al. (2016). Autochthony, allochthony and the role of consumers in influencing the sensitivity of aquatic systems to nutrient enrichment. *Food Webs, 7*, 1-12.

Yvon-Durocher, G., Caffrey, J. M., Cescatti, A., Dossena, M., del Giorgio, P., Gasol, J. M., et al. (2012). Reconciling the temperature dependence of respiration across timescales and ecosystem types. *Nature, 487*(7408), 472-476.

Appendix

Appendix. Methods

Periphyton Production

Periphyton production was measured in-situ at the Rice Rivers Center pier on 5 occasions between May-August 2016 to determine the periphyton contribution to pelagic metabolism. Periphyton production was measured in triplicate at 0.5 and 1.0 m depth intervals using horizontally placed unglazed clay tiles. Incubations lasted between 7-14 days, after which, periphyton were removed for CHLa analysis. CHLa samples were filtered through Whatman GF/A glass fiber filters following each periphyton incubation. Samples for pigment analysis were extracted in a 90% buffered acetone solution for 18 hours and analyzed on a Turner Design TD-700 Fluorometer (Sellers and Bukaveckas 2003, Bukaveckas et al. 2011). Areal periphyton CHLa abundance was then compared to areal pelagic CHLa abundance.

Zooplankton Dynamics

Macro (> 64 µm) and meso (64-20 µm) zooplankton samples were collected between March 2013 and December 2016 at a long-term Chesapeake Bay Program monitoring station (JMS75) located in the lower TF segment near the VCU RRC. Samples were collected twice per month when water temperatures > 10 °C and once per month when < 10 °C. All samples were collected in triplicate and preserved in a 5% acid Lugol's solution. Macrozooplankton (i.e., Copepods and Cladocerans) were collected via vertical tows (0-3m) with a 64 µm mesh plankton net equipped with a flowmeter. Mesozooplankton (i.e., Rotifers) were collected by filtering 20 L of water through a 20 µm mesh plankton net. A 5-20 mL subsample of each replicate was analyzed via microscopy at 40x (macrozooplankton) and 63x (mesozooplankton) magnification. Typically, ~50 individual macrozooplankton and ~100 individual mesozooplankton were

identified per subsample. Zooplankton abundance estimates were derived based on volume filtered and fraction of sub-sampled counted. Statistical analysis of these data used path analysis, a form of structural equation modeling (SEM; IBM Corp. Version 23.0), to determine the effect of multiple correlated variables on zooplankton abundance. Variables included in the model were: water temperature, freshwater replacement time (FRT), GPP, turbidity, CHLa, total suspended solids and particulate organic carbon. FRT was derived based on a date-specific method that divides the storage volume of the tidal fresh segment by the sum of preceding daily discharge measurements (Alber and Sheldon 1999). Discharge is continuously monitored by the USGS at sites near the Fall Line on the James (02037500) and Appomattox Rivers (02041650). Statistical significance among predictor variables was determined using an alpha ≤ 0.05. Model fitness, the chi-squared (χ^2) goodness-of-fit statistic, root mean square error of approximation (RMSEA) and the comparative fit index (CFI) (Hu and Bentler 1999). Models with the lowest χ^2 were determined to have better model fit, as well as a greater RMSEA score and a CFI approaching 1.

Appendix. Results

Pelagic Metabolism

Pelagic GPP and R were greater in the lower tidal freshwater (TF) segment of the James in comparison to the upper TF segment (Appendix Fig. 1). Pelagic GPP in the lower TF segment was nearly 10-fold higher (mean = 4.53 ± 0.57 g O_2 m^{-2} d^{-1}) relative to the upper TF (mean = 0.50 ± 0.22 g O_2 m^{-2} d^{-1}). Pelagic respiration was also higher in the lower TF segment (mean = 3.28 ± 0.42 g O_2 m^{-2} d^{-1}) in comparison to the upper TF (mean = 0.08 ± 0.01 g O_2 m^{-2} d^{-1}). Net pelagic metabolism was 3-fold higher in the lower TF segment (mean = 1.24 ± 0.33 g O_2 m^{-2} d^{-1}) relative to the upper TF segment (mean = 0.41 ± 0.21 g O_2 m^{-2} d^{-1}). Positive mean values

indicate that the water column was overall net autotrophic (GPP > R), though net heterotrophy was observed on some dates in Fall and Winter.

Light availability was an important determinant of pelagic GPP, particularly during periods of elevated water temperature (Appendix Fig. 2). When water temperatures were > 20 °C, instantaneous photosynthetically active radiation (PAR) explained 49% of the variation in pelagic GPP in the upper TF segment ($p = 0.0001$) and 77% of the variation in the lower TF segment ($p < 0.0001$). When water temperatures were < 20 °C, instantaneous PAR explained 19% of the variation in pelagic GPP in the upper TF segment ($p = 0.0001$) and 42% in the lower TF segment ($p < 0.0001$). Pelagic GPP had a significant positive linear relationship with pelagic R in the upper and lower TF segments of the James (Appendix Fig. 3). Pelagic GPP accounted for 48% of the variation in pelagic R for the upper TF segment ($p < 0.0001$) and 65% in the lower TF segment ($p < 0.0001$).

Periphyton Production

Periphyton production in the lower tidal freshwater segment of the JRE was routinely less than 1% of pelagic production. Areal pelagic CHLa concentration ranged between 15.4 and 5.8 µg cm^{-2} while areal periphyton CHLa concentration was always < 0.1 µg cm^{-2}. These results suggest that periphyton production contributes little to pelagic production, suggesting rapid light attenuation in the lower TF segment of the JRE.

Zooplankton Dynamics

Macrozooplankton from the lower tidal freshwater segment of the JRE were dominated by the cladoceran *Bosmina longirostris* and the copepod *Eurytemora affinis* during the study period. Mesozooplankton from the same segment were dominated by rotifers (principally *Brachionus*, *Kelicottia* and *Keratella*) and copepod nauplii. All zooplankton abundance showed

seasonal variation with lower abundances during the winter months and greater abundances in summer months (Appendix Fig. 4). Rotifers were most abundant during the study period averaging 421,439 ± 44,016 ind. m^{-3}, followed by copepod nauplii (769 ± 212 ind. m^{-3}) which were on average significantly ($p < 0.001$) more abundant during the study period than *Bosmina* and *Eurytemora* (312 ± 93 and 274 ± 78 ind. m^{-3} respectively). Peek *Bosmina* abundances succeed peeks in *Eurytemora* which succeeded peeks in copepod nauplii abundance. Rotifer abundance persisted at elevated levels when water temperature was greater than 13 °C.

The best fitting model for each zooplankton had the same model structure and variables, with water temperature and FRT as abiotic variables and GPP, POC and turbidity as biotic variables (Appendix Fig. 5). Each model had significant and positive relationships between FRT and POC concentration ($p < 0.001$), water temperature and POC concentration ($p = 0.002$) and water temperature and GPP ($p < 0.001$; Appendix Fig. 5). *Bosmina* abundance was directly and positively correlated with FRT which explained 36% of the variation in *Bosmina* abundance ($p < 0.001$; Appendix Fig. 5a). The path analysis model for *Bosmina* explained ~38% of the total variation in *Bosmina* abundance ($R^2 = 0.38$; Appendix Fig. 5a). *Eurytemora* abundance was not well constrained by the path analysis ($R^2 = 0.10$) with no significant direct effects of any variable on *Eurytemora* abundance (Appendix Fig. 5b). Copepod nauplii abundance was directly and positively correlated with turbidity ($p = 0.028$) with the model explaining 20% of the total variation in copepod nauplii abundance ($R^2 = 0.20$; Appendix Fig. 5c). Total rotifer abundance was directly and positively correlated with increasing water temperature ($p = 0.003$; Appendix Fig. 5d). The path analysis model for total rotifer abundance explained 48% of the total variation in rotifer abundance ($R^2 = 0.48$; Appendix Fig. 5d).

Appendix. Figures

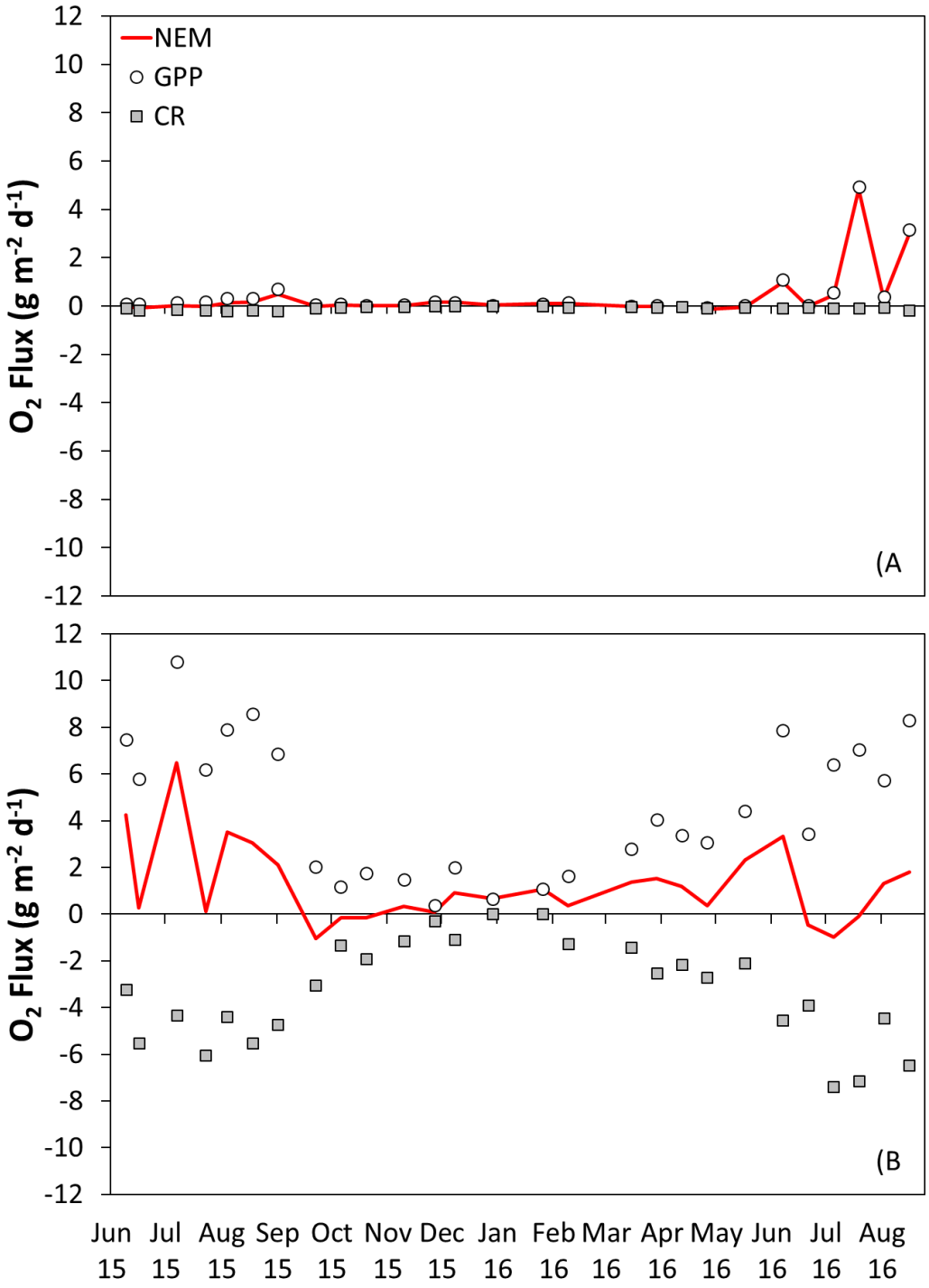

Appendix Figure 1. Pelagic gross primary production (GPP), community respiration (CR) and net ecosystem metabolism (NEM) from the upper (A) and lower TF (B) segments of the James River Estuary.

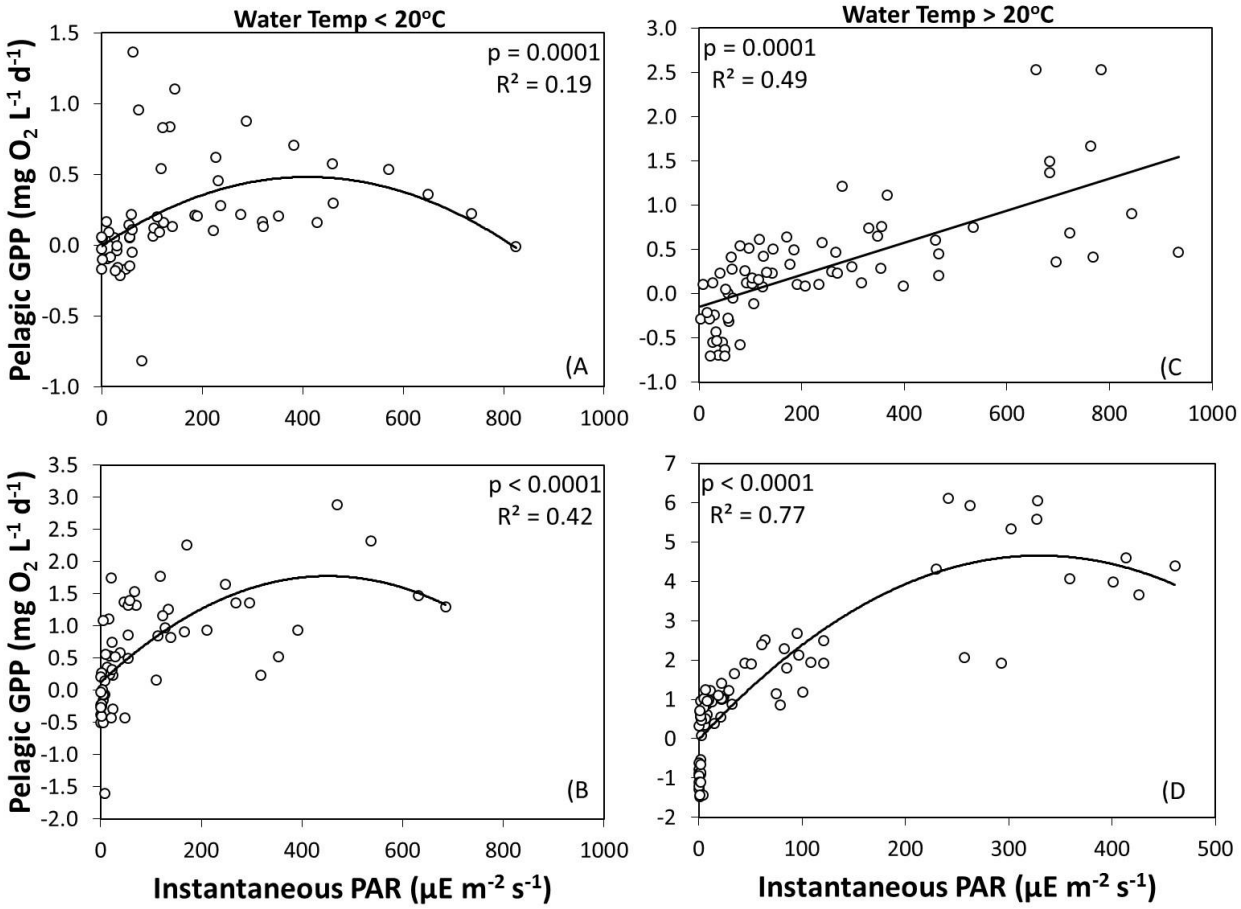

Appendix Figure 2. Production (pelagic GPP) versus irradiance curves for the upper (A, C) and lower TF (B, D) segments of the James River Estuary when water temperature was above or below 20 ^{o}C.

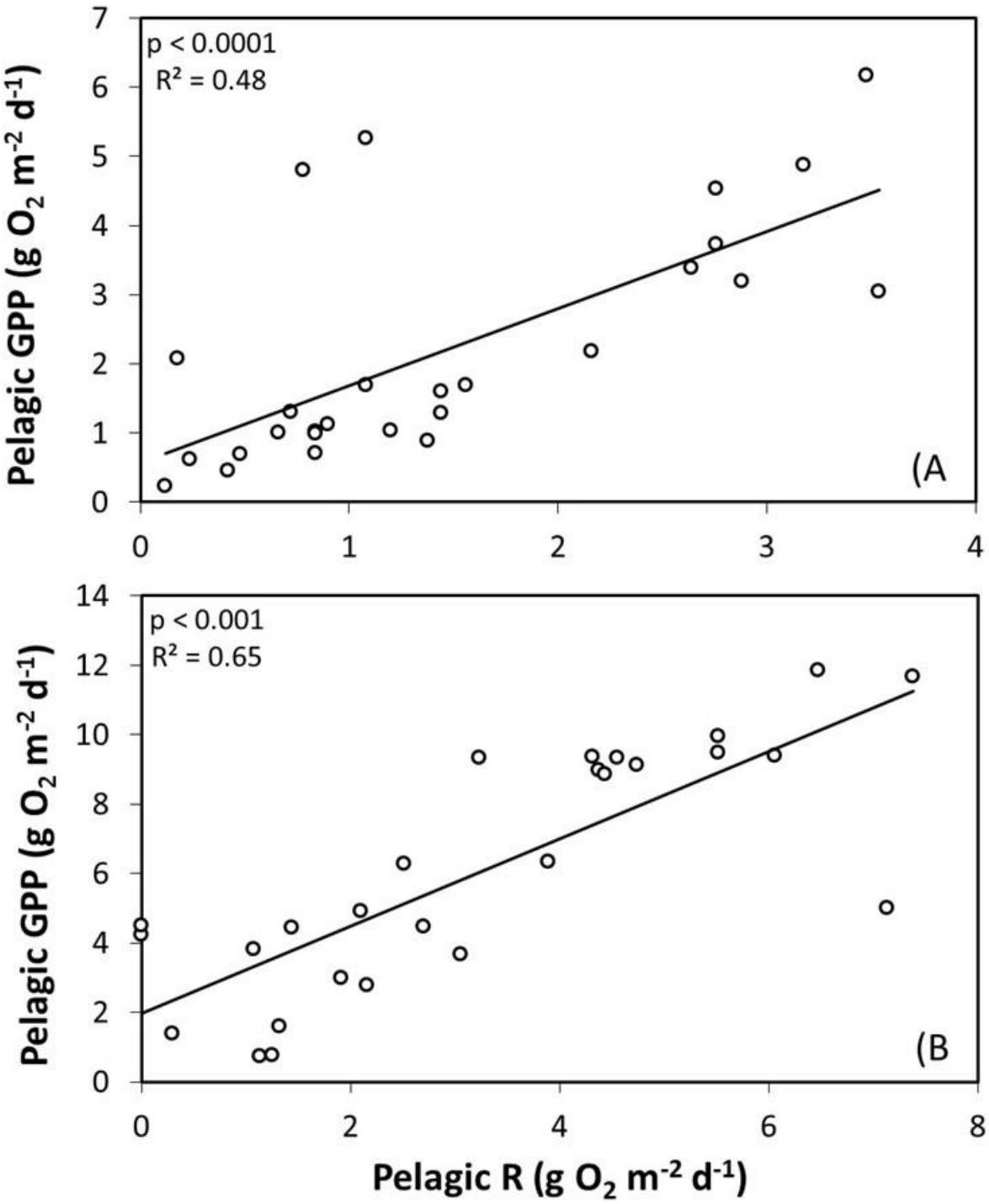

Appendix Figure 3. Pelagic R had a significant positive linear relationship with pelagic GPP in the upper TF (A) and lower TF (B) segments of the James River.

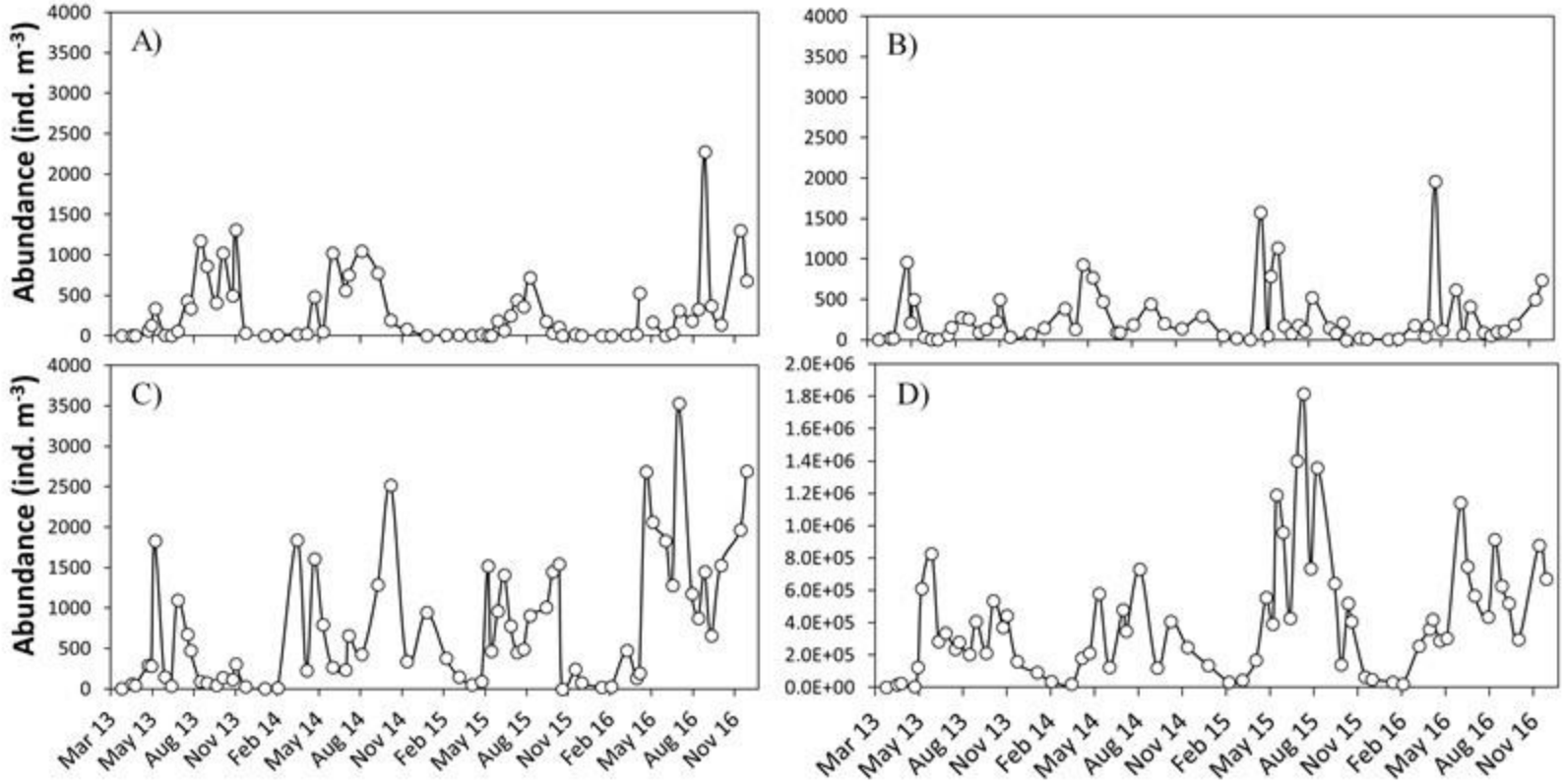

Appendix Figure 4. Densities of *Bosmina longirostris* (A), *Eurytemora affinis* (B) Copepod nauplii (C) and all rotifers (D) during 2013-2016 at station JMS75 located in the lower TF segment of the James River.

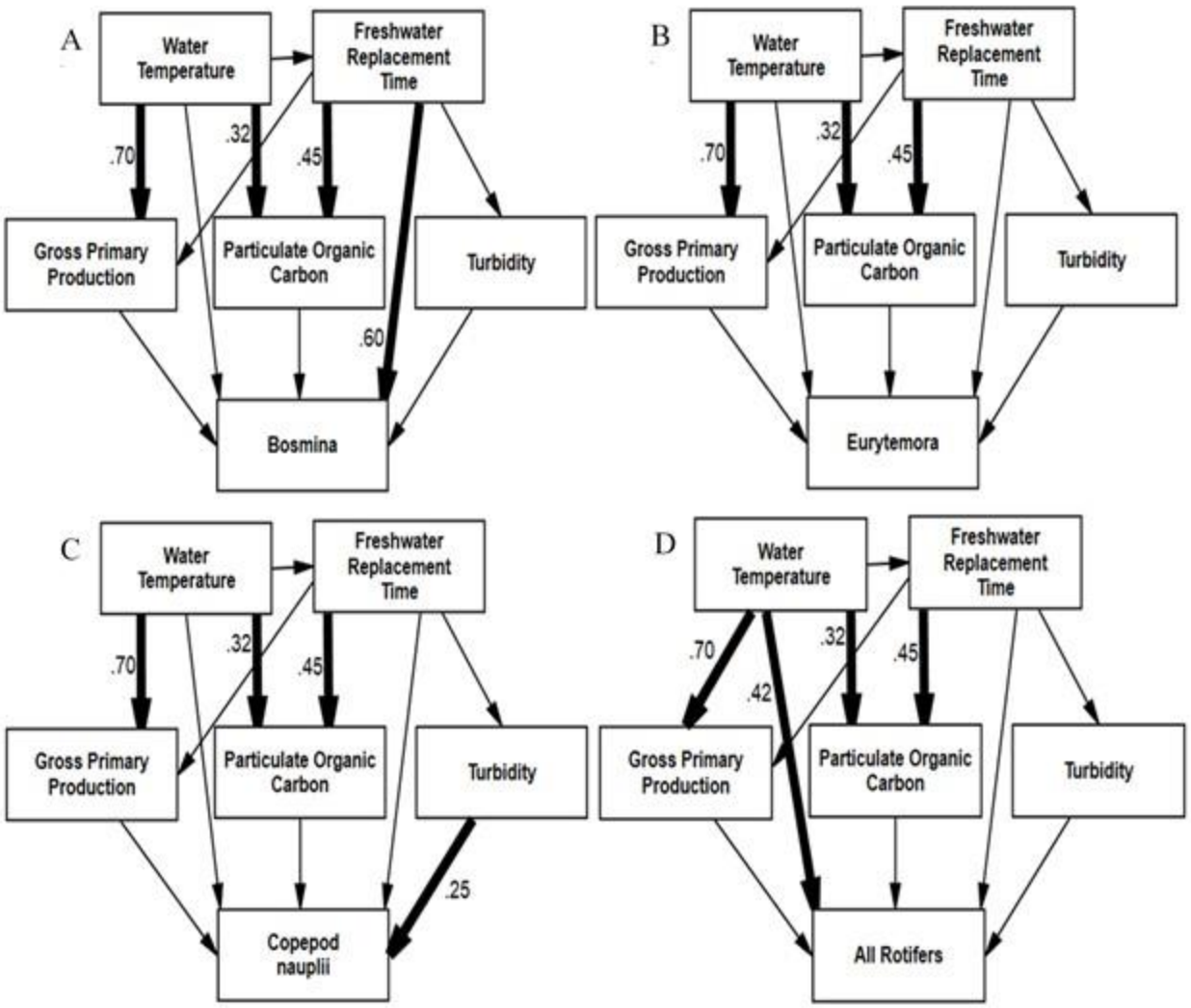

Appendix Figure 5. Path analysis results for models predicting temporal variation in the abundance of *Bosmina longirostris* (A), *Eurytemora affinis* (B) Copepod nauplii (C) and all rotifers (D) in the lower TF segment of the James River. Bold lines denote statistically significant ($p < 0.05$) pathways and values denote the correlation coefficient of each statistically significant pathway.